



## Calculated site substitution in ternary gamma'-Ni<sub>3</sub>Al: Temperature and composition effects

Ruban, Andrei; Skriver, Hans Lomholt

*Published in:*  
Physical Review B

*Link to article, DOI:*  
[10.1103/PhysRevB.55.856](https://doi.org/10.1103/PhysRevB.55.856)

*Publication date:*  
1997

*Document Version*  
Publisher's PDF, also known as Version of record

[Link back to DTU Orbit](#)

*Citation (APA):*  
Ruban, A., & Skriver, H. L. (1997). Calculated site substitution in ternary gamma'-Ni<sub>3</sub>Al: Temperature and composition effects. *Physical Review B*, 55(2), 856-874. <https://doi.org/10.1103/PhysRevB.55.856>

---

### General rights

Copyright and moral rights for the publications made accessible in the public portal are retained by the authors and/or other copyright owners and it is a condition of accessing publications that users recognise and abide by the legal requirements associated with these rights.

- Users may download and print one copy of any publication from the public portal for the purpose of private study or research.
- You may not further distribute the material or use it for any profit-making activity or commercial gain
- You may freely distribute the URL identifying the publication in the public portal

If you believe that this document breaches copyright please contact us providing details, and we will remove access to the work immediately and investigate your claim.

## Calculated site substitution in ternary $\gamma'$ -Ni<sub>3</sub>Al: Temperature and composition effects

A. V. Ruban and H. L. Skriver

*Center for Atomic-scale Materials Physics and Department of Physics, Technical University of Denmark, DK-2800 Lyngby, Denmark*

(Received 2 August 1996)

The temperature and composition dependence of the site substitution behavior of ternary additions to Ni<sub>3</sub>Al is examined on the basis of first-principles calculations of the total energies of ternary, partially ordered ( $\gamma'$ ) alloys. The calculations are performed by means of the linear muffin-tin orbitals method in conjunction with the local-density and multisublattice coherent-potential approximations and include all 3d, 4d, 5d, and noble metals. The calculations show the existence of simple trends in the alloying behavior of the  $\gamma'$  phase which may be explained in a Friedel-like model based on the interaction between Ni and the added species. It is shown that the commonly accepted interpretation of the site substitution behavior of Cu and Pd may be incorrect because of site substitution reversal at high temperatures. It is further shown that the direction of the solubility lobe in the ternary phase diagram for the elements Co, Pd, Cu, and Ag incorrectly has been interpreted as evidence for strong Ni site preference and that, in fact, these elements are expected to exhibit only weak Ni site preference. [S0163-1829(97)03902-7]

### I. INTRODUCTION

Intermetallic compounds which are ordered at high temperatures and which preserve a large amount of long-range order (LRO) up to the melting point are promising materials in technological fields ranging from the development of new types of catalysts to the creation of a new generation of high-temperature superalloys for the aircraft industry. Similar to the case of pure metals, the mechanical properties of pure compounds, without any additions, are usually poor and must be improved, for instance by a substitutional alloying which affects the physical properties at the atomic level. The alloying behavior of intermetallic compounds is therefore a subject not only of great practical interest but also of fundamental theoretical interest. This is particularly true because the existence of two or more different sublattices leads to new physical phenomena connected with the possibility of site selectivity of the alloying species. In addition, it is a great challenge to study these phenomena from first-principles, i.e., electronic structure calculations.

One of the most well-known examples of such an intermetallic compound is  $\gamma'$ -Ni<sub>3</sub>Al and the first attempts to understand its alloying behavior were made by Guard and Westbrook in 1959.<sup>1</sup> Based on the analysis of ternary phase diagrams these authors formulated several simple rules connecting the alloying behavior of the  $\gamma'$  phase to the electronic configuration and atomic size of the alloying elements. In particular, they found that the elements closest in size to either nickel or aluminum had the greatest solubility, and they suggested that the site substitution behavior of ternary additions to Ni<sub>3</sub>Al, which they deduced from the direction of the solubility lobe of the  $\gamma'$  phase in ternary phase diagram, was governed by the electronic structure of the ternary addition rather than by the atomic size factor.

Sixteen years later Rawlings and Staton-Bevan<sup>2</sup> established the existence of a strong correlation between the site occupation of the ternary additions and the mechanical properties of the  $\gamma'$  phase. Following this pioneering work there have appeared a number of experimental investigations of

site occupation using a large variety of different techniques, such as x-ray diffractometry,<sup>3-5</sup> transmission electron microscopy,<sup>5,6</sup> atom probe field ion microscopy,<sup>7,8</sup> ion channeling, and nuclear reaction analysis.<sup>9-11</sup> As a result of the experimental efforts it is now believed that Co, Cu, and Pd occupy only Ni sites in Ni<sub>3</sub>Al and that Ti, V, and Nb occupy only Al sites. For all other alloying elements the experimental data or their interpretation is either uncertain or even contradictory.

The theoretical investigation of the alloying behavior of  $\gamma'$ -Ni<sub>3</sub>Al has mainly been centered around considerations of the site preference of ternary additions.<sup>12-18</sup> Almost all the work has been based on the application of phenomenological Ising-type models which have turned out to be very useful in formulating and clarifying the problem. In this regard, we particularly want to mention the work of Wu *et al.*<sup>14</sup> who modeled the site occupation in *L1*<sub>2</sub> ordered intermetallics in terms of nearest neighbor effective pair interactions. Based on the simplest Ising Hamiltonian these authors found by means of the cluster variation method (CVM) that (i) at finite temperatures the site substitution behavior is not generally related to the direction of the solubility lobe and (ii) the site preference may change with the alloy composition and temperature. These conclusions have been overlooked in a number of subsequent experimental and theoretical investigations, and the neglect has led to misinterpretations of experimental data.

Wolverton and de Fontaine<sup>17</sup> determined the site preference of a number of ternary additions to Ni<sub>3</sub>Al on the basis of nearest neighbor effective pair interactions derived from electronic structure calculations. Subsequently, Sluiter *et al.*<sup>18</sup> applied an analogous as well as a supercell technique to calculate the site substitution behavior of 27 elements from the third, fourth, and fifth row of the Periodic Table. Thereby, these authors established the existence of a simple trend in the site substitution behavior of the 3d-transition metals, i.e., increasing Ni-site preference as a function of atomic number, which in general agreed with experimental data.

In spite of considerable theoretical efforts a number of problems still remain to be resolved. First of all, previous first-principles calculations<sup>17,18</sup> treated only some of the 4d and none of the 5d transition metals although these are the most important alloying elements used to improve the mechanical properties of  $\gamma'$ -Ni<sub>3</sub>Al. In addition, they are the elements for which the experimental data is the most controversial. Secondly, the first-principles calculations did not include temperature and composition effects which may strongly influence the site substitution behavior of the ternary additions and therefore are of vital importance for a correct interpretation of experimental data.

To address the outstanding questions we determine in the present work the site substitution behavior of all transition and noble metals in Ni<sub>3</sub>Al at 0 K from an empirical parametrization of the ordering energy obtained in first-principles calculations of the total energy of ternary, partially ordered alloys by means of the coherent potential approximation (CPA) in conjunction with the linear muffin-tin orbitals (LMTO) method in the tight-binding (TB) representation.<sup>19</sup> This approach has the advantage that it does not rely on perturbation theory or effective pair interactions and it leads to a physically transparent classification of site-occupation in Ni<sub>3</sub>Al in terms of a single parameter.

A brief account of our total energy calculations and the corresponding classification of the site-substitution behavior has been given in Ref. 20. Here, we first present a complete theory of ternary additions to an ordering binary alloy and we use the total energy calculations to derive a model for site substitution in Ni<sub>3</sub>Al which is the analogue of the rectangular *d*-band model of the cohesive energy developed by Friedel.<sup>21</sup> In addition, we consider for selected elements the influence of alloy composition and temperature on the site substitution behavior within the single-site mean-field approximation as well as in the framework of the cluster variation method with interatomic interactions deduced from the parametrized ordering energy. Finally, we calculate the enthalpies of formation of ternary  $\gamma'$  phases which enables us to estimate the possible directions of solubility lobes of  $\gamma'$  in a number of ternary phase diagrams at low temperatures.

In the present approach, the electronic structure of partially ordered alloys is computed within the CPA. Hence we neglect short range order (SRO) effects on the sublattices and local lattice relaxation effects in the form of displacements of the atomic species from their ideal positions on the underlying lattice due to the size difference of the alloy components. In concentrated, random alloys the neglect of these two effects may lead to an inadequate description of the thermodynamic properties of real random alloys.<sup>19,22,23</sup> However, as we shall now explain, both effects may safely be neglected when we consider a high-temperature ordering intermetallic compound with a small amount of ternary alloying element.

At ambient temperatures the long-range order parameters of a high-temperature ordering compound are close to 1 and therefore the random alloy on each sublattice may be considered dilute. In that case, the contribution from short-range order effects to the total energy of the compound is of order  $c^2$ , where  $c$  is the small concentration of the foreign element on a sublattice, and may be neglected in comparison with all other contributions to the total energy which are of order  $c$ .

Furthermore, it has been shown by Krivoglaz<sup>24</sup> that also the entropy contribution from correlations or SRO effects to the free energy of such alloys may be neglected.

In spite of the fact, that the local lattice relaxations vanish in a pure metal or a completely ordered compound, their effect may be large even in the case of a single, isolated impurity or an antisite defect. However, in a high-temperature ordering intermetallic compound their contribution to the energetics is typically one order of magnitude smaller than the unrelaxed defect energy. Estimates of the energy of local relaxations in random substitutional alloys range from 0 to 0.2 eV,<sup>22,25</sup> depending on the atomic size difference and bulk moduli of the alloy components, while the formation energy of antisite defects in such compounds is not less than 1 eV. Since the site preference of a ternary addition is determined by the difference in impurity energies and since the local environment of the Ni and Al sublattices are rather similar the contributions from the local relaxations to the site occupation tend to cancel. Thus, although short range order effects and local relaxations are present in Ni<sub>3</sub>Al they are unimportant in the study of site preference.

## II. ORDER PARAMETERS AND CONFIGURATION SPACE

In the present work we shall consider a binary, ordered alloy  $A_k B_m$  with two types of sublattices where the  $k$   $A$  sublattices as well as the  $m$   $B$  sublattices are considered to be equivalent. We shall furthermore assume that the ternary additions to this alloy do not cause a phase transition and that the symmetry of the binary host therefore is preserved. The distribution of the elements between sublattices in such a ternary phase may be determined by two long-range order (LRO) parameters which we define as

$$\begin{aligned}\eta_A &= c_A(A) - c_A(B), \\ \eta_B &= c_B(B) - c_B(A).\end{aligned}\quad (1)$$

Here,  $c_\kappa(\alpha)$  is the atomic fraction of the  $\kappa$  element on the  $\alpha$  sublattice which, in turn, may be expressed in terms of  $\eta_\kappa$  and the concentration  $\bar{c}_\kappa$  of the  $\kappa$  element in the alloy, i.e.,

$$\begin{aligned}c_A(A) &= \bar{c}_A + \xi_B \eta_A, \\ c_B(B) &= \bar{c}_B + \xi_A \eta_B, \\ c_A(B) &= \bar{c}_A - \xi_A \eta_A, \\ c_B(A) &= \bar{c}_B - \xi_B \eta_B, \\ c_X(A) &= \bar{c}_X - \xi_B (\eta_A - \eta_B), \\ c_X(B) &= \bar{c}_X + \xi_A (\eta_A - \eta_B),\end{aligned}\quad (2)$$

and

$$\xi_A = \frac{k}{k+m}; \quad \xi_B = \frac{m}{k+m}. \quad (3)$$

It follows from Eq. (2) that the distribution of species between sublattices upon a ternary addition to an alloy with

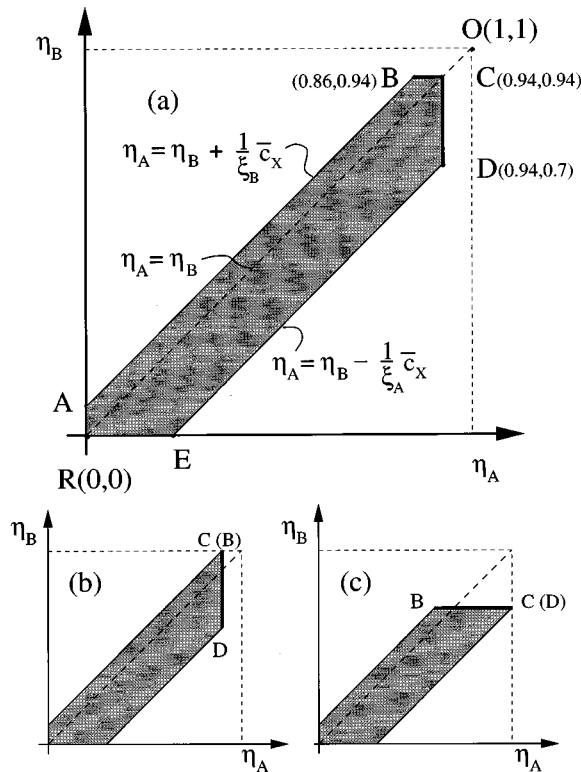


FIG. 1. Configurational space of LRO parameters (shaded areas) for the ternary  $A_3B(X)$  alloy with (a) equideficient  $A_{70.5}B_{23.5}X_6$ , (b) A-deficient  $A_{69}B_{25}X_6$ , and (c) B-deficient  $A_{75}B_{19}X_6$  compositions. Segments  $BC$  and  $CD$  are the points of the maximally ordered states.  $R$ , i.e.,  $(0,0)$ , is the point of the completely random state and  $O$ , i.e.,  $(1,1)$ , the point of the completely ordered state. Note, that point  $C$  is on the line  $\eta_A = \eta_B$  only for equideficient ternary alloy compositions.

a particular composition  $(\bar{c}_A, \bar{c}_B)$  may be mapped onto the configuration space defined by the LRO parameters  $(\eta_A, \eta_B)$ . Further, as shown in Fig. 1 each alloy has its own configuration space defined by the polygon of possible values of the LRO parameters determined by the condition  $c_\kappa(\alpha) \geq 0$  for all  $\kappa$  and  $\alpha$ . In the case of a binary alloy  $A_kB_m$ , i.e.,  $\bar{c}_X = 0$ , the configuration polygon degenerates into the straight line  $\eta_A = \eta_B$  which connects the point of the completely random state  $\eta_A = \eta_B = 0$ ,  $R$  in Fig. 1, with that of the maximally ordered state. For a stoichiometric alloy where  $\bar{c}_A = \xi_A$  and  $\bar{c}_B = \xi_B$  the latter corresponds to the completely ordered state  $\eta_A = \eta_B = 1$ ,  $O$  in Fig. 1. In the off-stoichiometric case where, for instance,  $\bar{c}_A > \xi_A$  the point of the maximally ordered state is  $\eta_A = \eta_B = (1 - \bar{c}_A)\xi_B$ .

To characterize the maximally ordered state in terms of atomic redistribution we shall distinguish between two type of antisite defects. The first is a *partial* antisite defect created by the transfer of one alloy component to the sublattice of opposite type. The second is an *exchange* antisite defect created by the exchange of atoms of opposite type between sublattices in such a way that they create simultaneously two partial antisite defects on each sublattice. In a binary alloy it is impossible to create a single partial antisite defect at a fixed alloy composition unless a vacancy is created on the other sublattice. They may, however, be created in pairs accompanied by the opposite partial antisite defects, i.e., as

exchange antisite defects, as the temperature increases.

It follows that the maximally ordered state may be defined as the state without any exchange antisite defects. In a stoichiometric alloy it is therefore the completely ordered state without any partial antisite defects, while in an off-stoichiometric alloy there must be a number of partial antisite defects either on the  $A$  or on the  $B$  sublattices which do not have their counterparts on the other sublattice. The maximally ordered state of an alloy, which will order, is the state of lowest energy at 0 K for fixed lattice structure and symmetry. This is so because the energy of forming an exchange antisite defect must be positive in this case, and therefore the only way to create exchange antisite defects is to heat up the alloy. The increasing number of exchange antisite defects corresponds to a change of the order parameters along the line  $\eta_A = \eta_B$  towards the point  $(0,0)$  in the configuration space of the alloy.

The addition of a third element to a binary, ordered phase expands the available configuration space from the line  $\eta_A = \eta_B$  of the binary alloy to a polygon of finite width  $\bar{c}_X/(\xi_A\xi_B)$  bounded by

$$\eta_A = \eta_B - \frac{1}{\xi_A}\bar{c}_X,$$

$$\eta_A = \eta_B + \frac{1}{\xi_B}\bar{c}_X, \quad (4)$$

and the maximum values of the order parameters to be discussed below. The state of the ternary alloy may therefore leave the line  $\eta_A = \eta_B$  which corresponds to the creation of defects connected with the distribution of the third alloying element on the sublattices. As a consequence partial antisite defects may be created at a fixed alloy composition without their counterparts by the exchange of ‘‘host’’ atoms with the ternary addition  $X$ . This means that a ternary alloy, in contrast to a binary alloy, has an infinite number of maximally ordered states, i.e., states without exchange antisite defects, and that any of these states may be the state of lowest energy at 0 K. Which state has the lowest energy depends on the nature of the alloying elements and external parameters, and constitutes the problem of site occupation behavior of a ternary addition.

In the LRO configuration space the points corresponding to the maximally ordered state are the points of the polygon of possible values for which at least one LRO parameter reaches its maximum value. The reason is that any change in the order parameters from larger to smaller values parallel to the line  $\eta_A = \eta_B$  corresponds to the creation of exchange antisite defects which in an ordering alloy is energetically unfavorable. The maximum values of the order parameters depend on the alloy composition but for compositions obeying the following conditions:

$$\bar{c}_A \leq \xi_A; \quad \bar{c}_B \leq \xi_B, \quad (5)$$

which define what may be called *quasistoichiometric* ternary alloy compositions in analogy to the stoichiometric compositions of binary alloys the maximum values of the LRO parameters are

$$\eta_A^{\max} = \bar{c}_A \frac{1}{\xi_A}; \quad \eta_B^{\max} = \bar{c}_B \frac{1}{\xi_B}. \quad (6)$$

For ternary off-stoichiometric compositions where one of the conditions (5) is not obeyed, e.g.,  $\bar{c}_A > \xi_A$ , the maximum values of the corresponding order parameters is determined by  $\eta_A^{\max} = (1 - \bar{c}_A)/\xi_B$  similar to the case of binary off-stoichiometric alloys.

In Fig. 1 we show the order parameter space for the ternary  $A_3B(X)$  alloy with three different alloy compositions:  $A_{70.5}B_{23.5}X_6$ ,  $A_{69}B_{25}X_6$ , and  $A_{75}B_{19}X_6$  corresponding to different  $\bar{c}_A/\bar{c}_B$  ratios at fixed concentration of the  $X$  component. The last two compositions for which  $\bar{c}_A/\bar{c}_B < k/m$  and  $\bar{c}_A/\bar{c}_B > k/m$  are so-called  $A$ - and  $B$ -deficient alloys, respectively, while the first composition where  $\bar{c}_A/\bar{c}_B = k/m$  we will call an *equideficient* ternary alloy. The maximally ordered states corresponds to the line segments  $BC$  and  $CD$  which may degenerate into a single point if  $\bar{c}_A \geq \xi_A$  or  $\bar{c}_B \geq \xi_B$ , i.e., for the off-stoichiometric and the extreme quasistoichiometric ternary alloy compositions.

The distribution of the atomic species on the sublattice sites corresponding to a maximally ordered state may easily be found from Eq. (2). In the example in Fig. 1 point  $B$  corresponds to the distribution of the alloy components where all the  $X$  atoms are on the  $A$  sublattice while point  $D$  corresponds to the case where all the  $X$  atoms are on the  $B$  sublattice and some  $B$  atoms have moved to the  $A$  sublattice thereby creating partial antisite defects. A change in configuration from  $C$  to  $D$ , or parallel to the line  $\eta_A = \text{const}$ , corresponds to the creation of partial antisite defects on sublattice  $B$  and substitutional defects of  $X$  atoms on sublattice  $A$  with a fixed number of  $A$  atoms on both sublattices. A change in order parameter parallel to the line  $BC$  of constant ( $\eta_B$ ) corresponds to a simultaneous creation or annihilation of substitutional defects on the  $B$  sublattice and partial antisite defects on the  $A$  sublattice. This means that there are no partial antisite defects in the quasistoichiometric ternary alloy corresponding to  $C$  where both order parameters reach their maximal value.

The experimental data and theoretical results concerning the distribution of a ternary addition  $X$  on the sublattices are usually given in terms of the fraction of  $X$  on one of the sublattices. For instance, the fraction of  $X$  in the  $B$  sites is given by

$$f = \frac{mc_X(B)}{mc_X(B) + kc_X(A)} = \xi_B + \frac{1}{\bar{c}_X} \xi_A \xi_B (\eta_A - \eta_B), \quad (7)$$

and, hence, constant along lines parallel to the line  $\eta_A = \eta_B$  on which it is equal to  $\xi_B$  which is also the value of  $f$  in the random state where both LRO parameters are equal to 0. Further,  $f = 0$  on the line  $AB$  as all  $X$  atoms are in the  $A$  sites and  $f = 1$  on the line  $DE$  as all  $X$  atoms are in the  $B$  sites. The fraction of  $X$  atoms in the  $B$  sites corresponding to the configuration point  $C$ , see Fig. 1, may be found from Eq. (6) to be given by

$$f(C) = \xi_B + \frac{1}{\bar{c}_X} (\xi_B \bar{c}_A - \xi_A \bar{c}_B). \quad (8)$$

Thus, for the equideficient alloy when the configuration point  $C$  is on the line  $\eta_A = \eta_B$  the fraction of  $X$  atoms in  $B$  sites is equal to  $\xi_B$ , i.e., the value for the random alloy.

### III. SITE PREFERENCE OF TERNARY ADDITIONS: DILUTE LIMIT

To determine the equilibrium distribution of the  $X$  element on the sublattice sites of the ordered binary phase  $A_kB_m$  at 0 K one must, in general, find that maximally ordered state which has the lowest internal or ordering energy. Since the possible, maximally ordered states depend on alloy composition it is more convenient to classify site preference of ternary additions as the site preference in the dilute limit  $\bar{c}_X \rightarrow 0$  for a quasistoichiometric ternary ordered phase at 0 K. In this case one can assume that initially the system is at point  $C$  of the configuration polygon, Fig. 1, i.e., that the  $X$  atoms are distributed among the  $A$  and  $B$  sublattice sites such that there are no partial antisite defects in the alloy. Note, that in the dilute limit  $C$  approaches the point of the completely ordered state (1,1).

In this dilute limit the  $X$  atoms have three possibilities at 0 K. First, they may move from the  $B$  sublattice to the  $A$  sublattice with the creation of partial antisite defects on the  $B$  sublattice. This corresponds to a change in state from  $C$  towards  $B$  in Fig. 1. Second, they may move from the  $A$  sublattice to the  $B$  sublattice creating partial antisite defects on the  $A$  sublattice, i.e., from  $C$  towards  $D$  in Fig. 1. Finally, they may remain in their positions, i.e., in state  $C$ . These possibilities lead to the following classification of the site substitution behavior of ternary additions to a binary ordered phase: (type I), strong  $A$ -site preference, (type II), strong  $B$ -site preference, and (type III), weak site preference.

To determine the site substitution behavior of a particular  $X$  element it is sufficient to determine the energies of two basic processes, i.e., that of moving a single  $X$  atom from a  $B$  site to an  $A$  site,  $E_{B \rightarrow A}^X$  and that of moving a single  $X$  atom from an  $A$  site to a  $B$  site,  $E_{A \rightarrow B}^X$ . We shall call these energies transfer energies. Neglecting the entropy contribution one finds at 0 K

$$\begin{aligned} E_{B \rightarrow A}^X(\eta_A, \eta_B) &= -\frac{1}{\xi_A \xi_B} \partial E_{\text{ord}}^X / \partial \eta_A \\ &= E^X(A) - E^X(B) + E_{\text{ant}}(B), \\ E_{A \rightarrow B}^X(\eta_A, \eta_B) &= -\frac{1}{\xi_A \xi_B} \partial E_{\text{ord}}^X / \partial \eta_B \\ &= E^X(B) - E^X(A) + E_{\text{ant}}(A), \end{aligned} \quad (9)$$

where  $E_{\text{ord}}^X(\eta_A, \eta_B)$  is the ordering energy, and the partial derivatives must be evaluated at the alloy configuration  $(\eta_A, \eta_B)$  under consideration. Further,  $E^X(A)$  and  $E^X(B)$  are the substitution energies of the ternary addition  $X$  on the  $A$  and  $B$  sublattices, respectively, and  $E_{\text{ant}}(A)$  and  $E_{\text{ant}}(B)$  the energies of the partial antisite defects on the  $A$  and  $B$  sublattices, respectively. It should be mentioned that these energies depend on the configurational state  $(\eta_A, \eta_B)$  at which they are determined. For instance, at (0,0),  $R$  in Fig. 1, which is the completely random state, they all vanish.

If  $E_{B \rightarrow A}^X$  is negative,  $X$  exhibits strong  $A$  site preference because in this case  $X$  atoms prefer to go to the  $A$  sublattice even at the cost of creating antisite defects on the  $B$  sublattice. This is type I behavior and means that at this particular point in the LRO space an  $X$  atom is more attracted to an  $A$  sublattice site than an  $A$  atom. Conversely, if  $E_{A \rightarrow B}^X$  is negative  $X$  exhibits strong  $B$  site preference, i.e., type II behavior. Finally, if both  $E_{B \rightarrow A}^X$  and  $E_{A \rightarrow B}^X$  are positive  $X$  exhibits weak site preference. In that case  $C$  is the state of lowest energy at 0 K because any change away from  $C$  will mean creation of antisite defects which is energetically unfavorable. This third group of the classification is naturally subdivided into type III(A), weak  $A$  site preference when  $E_{A \rightarrow B}^X > E_{B \rightarrow A}^X$  and type III(B) weak  $B$  site preference when  $E_{B \rightarrow A}^X > E_{A \rightarrow B}^X$ .

The two transfer energies  $E_{B \rightarrow A}^X$  and  $E_{A \rightarrow B}^X$  cannot both be negative. This follows upon addition of the equations (9) which gives

$$E_{B \rightarrow A}^X + E_{A \rightarrow B}^X = E_{\text{ant}}(B) + E_{\text{ant}}(A) = E_{\text{ant}}^{\text{xc}}, \quad (10)$$

where  $E_{\text{ant}}^{\text{xc}}$  is the energy of forming an exchange antisite defect which in the case of an ordering binary alloy must be positive. In general  $E_{\text{ant}}^{\text{xc}}$  depends not only on the alloy composition and the configurational state ( $\eta_A, \eta_B$ ) at which it is determined but also on the alloying element  $X$ . However, in the dilute limit of the ternary addition the latter dependence disappears.

The linear relation (10) between  $E_{B \rightarrow A}^X$  and  $E_{A \rightarrow B}^X$  allows one to describe the site substitution behavior in terms of a single parameter, e.g.,  $E_{B \rightarrow A}^X$ . Normalizing  $E_{B \rightarrow A}^X$  by the energy of the exchange antisite defect  $E_{\text{ant}}^{\text{xc}}$  which may be considered a natural unit of energy we find that the single parameter<sup>26</sup>

$$\tilde{E}_{B \rightarrow A}^X = E_{B \rightarrow A}^X / E_{\text{ant}}^{\text{xc}} \quad (11)$$

may be used to describe the site preference of ternary additions. The classification is then

- I:  $\tilde{E}_{B \rightarrow A}^X < 0$  (strong  $A$  site preference),
  - II:  $\tilde{E}_{B \rightarrow A}^X > 1$  (strong  $B$  site preference),
  - III(A):  $0 < \tilde{E}_{B \rightarrow A}^X < 0.5$  (weak  $A$  site preference),
  - III(B):  $0.5 < \tilde{E}_{B \rightarrow A}^X < 1$  (weak  $B$  site preference),
- (12)

which is completely analogous to the one established previously.<sup>12,14,16–18,20</sup> However, one should remember that this simple classification is only strictly valid for quasistochiometric ternary alloys in the dilute limit of the ternary addition and at 0 K. In fact, the site preference of a particular ternary addition may change with alloy composition and temperature.

#### IV. ORDERING ENERGY IN Ni<sub>3</sub>Al

To establish site substitution behavior according to the classification (12) one must compute the ordering energy  $E_{\text{ord}}^X$  and its derivatives (9) for each ternary  $3d$ ,  $4d$ , and  $5d$  addition to Ni<sub>3</sub>Al. This requires that we perform total

energy calculations for partially ordered Ni<sub>3</sub>Al with ternary additions and evaluate the ordering energy as the difference between the total energy  $E_{\text{tot}}$  of the partially ordered alloy and that of the completely random alloy, i.e.,

$$E_{\text{ord}}^X(\eta_{\text{Ni}}, \eta_{\text{Al}}) = E_{\text{tot}}(\eta_{\text{Ni}}, \eta_{\text{Al}}) - E_{\text{tot}}(0,0). \quad (13)$$

In the following we describe the computational technique used to obtain total energies and show that the number of first-principles calculations may be reduced by means of an empirical expansion of the ordering energy.

#### A. First-principles calculations

The necessary total energy calculations for partially ordered Ni<sub>3</sub>Al with ternary additions have been performed by means of the multisublattice linear muffin-tin orbitals (LMTO)-CPA method<sup>19</sup> in the scalar-relativistic, frozen core, and atomic sphere approximations (ASA) and in the tight-binding representation<sup>27–29</sup> with a minimal  $spd$  basis. For the pure elements and ordered Ni<sub>3</sub>Al we have used the LMTO-Green's function (GF) technique instead of solving the conventional Hamiltonian eigenvalue problem. All alloys and pure metals have been calculated in the  $L1_2$  structure.

The valence electrons were treated self-consistently within the local density approximation (LDA) with the Perdew-Zunger parametrization<sup>30</sup> of the results of Ceperley and Alder<sup>31</sup> for the exchange-correlation potential and energy. In the cases of Cr, Mn, Fe, and Co we have performed spin-polarized calculations in the local-spin density approximation with the Vosko-Wilk-Nusair parametrization.<sup>32</sup> Integration over the Brillouin zone has been performed by the special point technique<sup>33</sup> with 56  $\mathbf{k}$  points in the irreducible wedge (1/48th) of the simple cubic Brillouin zone. To calculate the off-diagonal elements of the Green's function which enters the CPA equation we applied the 48 proper symmetry operations of the  $L1_2$  structure to the Green's function calculated in the irreducible wedge (IBZ).

The individual atomic sphere radii were set equal to the average atomic Wigner-Seitz radius of the alloy. The moments of the state density needed for the kinetic energy and the valence charge density were calculated by integrating the Green's function on a complex energy contour using a Gaussian integration technique with 16 points on a semi-circle enclosing the occupied states. The convergence criteria for the total energy was 0.001 mRy. The equilibrium lattice parameter and corresponding ground state energy of a given alloy were obtained on the basis of 6 self-consistent calculations of the total energy close to the equilibrium lattice parameter and a subsequent fit to a Morse-type equation of state.<sup>34</sup>

The Madelung energy and potential were determined in the screened impurity model (SIM),<sup>19,35</sup> with a prefactor of  $\beta=0.6$  which makes the LMTO-CPA results for random Ni-Al alloys agree with those obtained by the Connolly-Williams method on the basis of the total energies of ordered alloys. Strictly speaking, the SIM should be modified in the case of ternary alloys by taking into account the possibility for  $\beta$  to be different in different binary alloys, i.e., Al-Ni, Al-X, and Ni-X. However, our experience shows that in the case of binary transition metal alloys the optimum value of

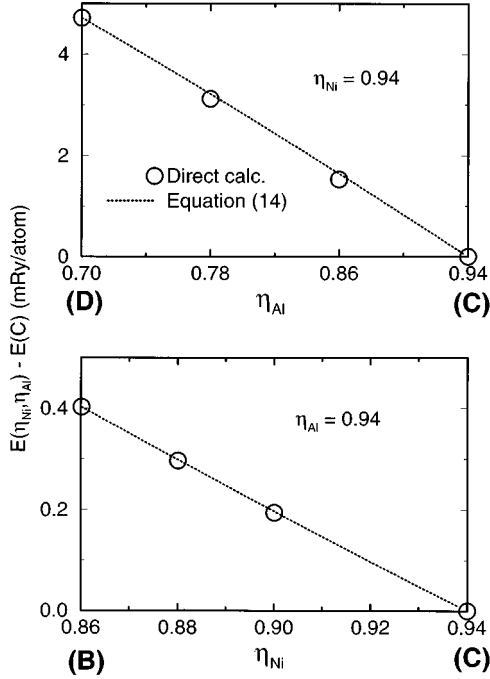


FIG. 2. The energies of the ternary partially ordered  $\text{Ni}_{70.5}\text{Al}_{23.5}\text{Co}_6$  alloy along the segments of the maximally ordered states  $BC$  and  $CD$  relative to the energy in point  $C$ , i.e.,  $\eta_{\text{Ni}} = \eta_{\text{Al}} = 0.94$ , (Fig. 1) calculated directly (open circles) and from Eq. (14).

$\beta$  varies only from 0.55 to 0.65 and therefore we expect a common  $\beta$  value to be a good approximation.

### B. Empirical expansion

The number of first-principles calculations needed to establish the site substitution behavior may be reduced by means of the quadratic expansion of the ordering energy

$$E_{\text{ord}}^X(\eta_{\text{Ni}}, \eta_{\text{Al}}) = U_{\text{Ni-X}} \eta_{\text{Ni}}^2 + U_{\text{Al-X}} \eta_{\text{Al}}^2 - 2U_{\text{Ni-Al-X}} \eta_{\text{Ni}} \eta_{\text{Al}}, \quad (14)$$

in terms of the order parameters. Although this appears to be an empirical expansion the expansion coefficients,  $U_{\text{Ni-X}}$ ,  $U_{\text{Al-X}}$ , and  $U_{\text{Ni-Al-X}}$ , may be related to effective pair interactions, or their Fourier components, of an Ising type model, as shown in Appendix A. In the present calculations the three expansion coefficients have been determined for each ternary addition  $X$  from the calculated total energies (13) of  $\text{Ni}_{70.5}\text{Al}_{23.5}\text{X}_6$  ternary alloys in the configurational states corresponding to the points (0.94,0.70), (0.94,0.94), (0.86,0.94), and (0,0) in the  $(\eta_{\text{Ni}}, \eta_{\text{Al}})$  space of LRO parameters. These states correspond to the points  $B$ ,  $C$ ,  $D$ , and  $R$  in Fig. 1 for  $A$  and  $B$  equal to  $\text{Ni}$  and  $\text{Al}$ , respectively.

We have tested the accuracy of the quadratic expansion (14) for a few ternary additions by comparison with total energy calculations (13) for additional points along  $BC$  and  $DC$  in Fig. 1 corresponding to the maximally ordered states. We find that in all cases (14) gives a very accurate description of the ordering energy as may be seen in Fig. 2 for  $X$  equal to  $\text{Co}$ . The validity of the quadratic expansion may be

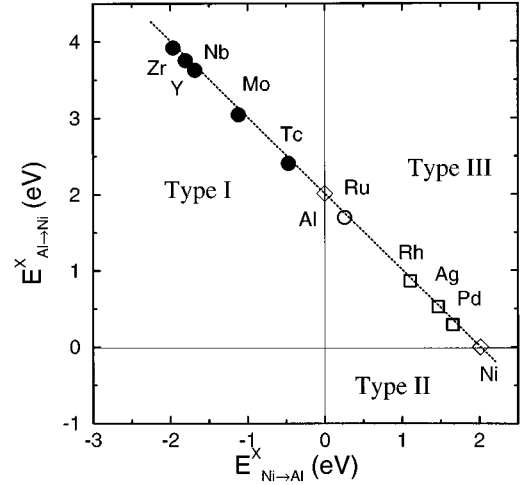


FIG. 3. The energies of moving ternary additions from  $\text{Ni}$  to  $\text{Al}$  sites  $E_{\text{Ni} \rightarrow \text{Al}}^X$  and from  $\text{Al}$  to  $\text{Ni}$  sites  $E_{\text{Al} \rightarrow \text{Ni}}^X$  defined at the point (1,1) of the LRO space on the basis of the ordering energies (14) of  $\text{Ni}_{70.5}\text{Al}_{23.5}\text{X}_6$  ternary alloys. The line  $E_{\text{Ni} \rightarrow \text{Al}}^X + E_{\text{Al} \rightarrow \text{Ni}}^X = E_{\text{ant}}^{\text{xc}}$  where  $E_{\text{ant}}^{\text{xc}} = 2.0$  eV is the energy of antisite defect formation of the completely ordered  $\text{Ni}_3\text{Al}$ . The filled circles are the additions with a strong preference (sufficient to create antisite defects) for occupation of  $\text{Al}$  sites (type I), open circles are the additions with a weak preference (insufficient to create antisite defects) for  $\text{Al}$  sites [type III ( $\text{Al}$ )] and open squares are the additions with a weak (insufficient to create antisite defects) preference for  $\text{Ni}$  sites. The open diamonds correspond to the substitution behavior of  $\text{Al}$  and  $\text{Ni}$  atoms as ternary additions.

seen as a consequence of the fact that in the case of  $\text{Ni}_3\text{Al}$  the next, triplet interactions, are shown to be smaller than pair interactions.<sup>25</sup>

Strictly speaking, the classification (12) is only valid for quasistoichiometric ternary alloys in the dilute limit of the ternary addition. One might therefore worry whether the concentration of the ternary additions, i.e., 6 at. %, used in the total energy calculations is sufficiently close to this dilute limit to yield concentration independent expansion coefficients  $U_{\text{Ni-X}}$ ,  $U_{\text{Al-X}}$ , and  $U_{\text{Ni-Al-X}}$ . To address this question we show in Fig. 3 the  $4d$  transfer energies  $E_{\text{Ni} \rightarrow \text{Al}}^X$  and  $E_{\text{Al} \rightarrow \text{Ni}}^X$  calculated from Eq. (9) by means of Eq. (14) evaluated in the dilute limit, i.e., for  $(\eta_{\text{Ni}}, \eta_{\text{Al}}) = (1,1)$ . In addition we show the antisite defect energy  $E_{\text{ant}}^{\text{xc}}$  calculated for pure, binary  $\text{Ni}_3\text{Al}$ , i.e., also completely in the dilute limit. This energy is labeled  $\text{Al}$  or  $\text{Ni}$  in Fig. 3. The fact that the transfer energies obey the linear relationship (10) to a high degree of accuracy and that the line cuts the axes at exactly the antisite energy determined for binary  $\text{Ni}_3\text{Al}$  strongly indicates that the calculated transfer energies indeed represent the dilute limit. We mention that the transfer energies of the  $5d$  metals obey exactly the same relationship and that the analogous plot for the  $3d$  metals including the effect of spin polarization may be found in Ref. 20.

The above results do not mean, however, that the composition dependence of the ordering energy itself may be neglected. In fact, we find that the positions of the points on the line  $E_{\text{Al} \rightarrow \text{Ni}}^X + E_{\text{Ni} \rightarrow \text{Al}}^X = E_{\text{ant}}^{\text{xc}}$  depend on the alloy composition, particularly if the ratio  $\bar{c}_{\text{Ni}}/\bar{c}_{\text{Al}}$  is changed. On the other hand, as also found by Sluiter *et al.*<sup>18</sup> for the effective pair

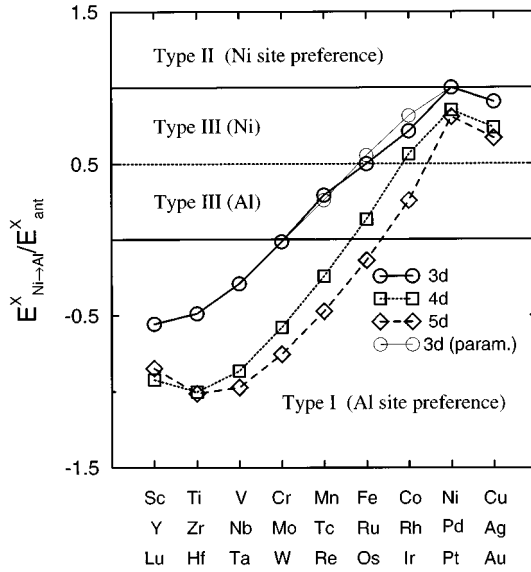


FIG. 4. Calculated transfer energy for the 3d, 4d, and 5d transition metals classified according to Eq. (12). The energy of antisite defect formation  $E_{\text{ant}}^X \approx 2.00$  eV. The thin symbols for 3d metals are the results of paramagnetic calculations.

interactions in ternary  $\text{Ni}_y\text{Al}_{1-y-x}\text{Fe}_x$  alloys, the changes are small and do not qualitatively influence the picture of the site substitution behavior of ternary additions presented below.

## V. SITE SUBSTITUTION IN $\text{Ni}_3\text{Al}$

### A. General trends

In Fig. 4 we present a unified picture of the site substitution behavior of ternary 3d, 4d, and 5d transition-metal additions to  $\text{Ni}_3\text{Al}$  in the dilute limit of quasistoichiometric ternary alloys at 0 K based on the classification (12)

$$\begin{aligned} \text{I: } & \tilde{E}_{\text{Ni} \rightarrow \text{Al}}^X < 0, \\ \text{II: } & \tilde{E}_{\text{Ni} \rightarrow \text{Al}}^X > 1, \\ \text{III(Al): } & 0 < \tilde{E}_{\text{Ni} \rightarrow \text{Al}}^X < 0.5, \\ \text{III(Ni): } & 0.5 < \tilde{E}_{\text{Ni} \rightarrow \text{Al}}^X < 1, \end{aligned} \quad (15)$$

where the transfer energies  $\tilde{E}_{\text{Ni} \rightarrow \text{Al}}^X$  and  $E_{\text{Ni} \rightarrow \text{Al}}^X$  are determined from the empirical expansion of the ordering energy at  $(\eta_{\text{Ni}}, \eta_{\text{Al}}) = (1, 1)$ .

In the figure one observes two trends which are obeyed by all metals but those at the very ends of the series. First, as the  $d$ -occupation number increases along a series the preference for Al sites decreases. Second, as the atomic number increases down a column the preference for Al sites increases. It is also seen that no element among the transition and noble metals is expected to occupy only Ni sites in  $\text{Ni}_3\text{Al}$ , i.e., exhibit type II behavior. Finally, we find that within the accuracy of our calculations  $E_{\text{Al} \rightarrow \text{Ni}}^{\text{Fe}} = E_{\text{Ni} \rightarrow \text{Al}}^{\text{Fe}}$  and, hence, Fe is the only addition which exhibits a “pure” type III behavior.

The results in Fig. 4 agree well with the available theoretical values obtained by Sluiter and Kawazoe<sup>18</sup> and in gen-

eral with the conclusions drawn from experimental data concerning site preference of ternary additions to  $\text{Ni}_3\text{Al}$ . The only exceptions appear to be Co, Cu, and Pd which according to experimental evidence are believed to exhibit strong Ni site preference, i.e., type II behavior, in contradiction to the calculated type III (Ni) classification. However, in the interpretation of the experimental results one has neglected the fact that all measurements of site preference have been performed at finite temperature and at some nondilute concentration. The reduction of such data to 0 K and to the dilute limit is not always trivial and must include the possibility of site-occupation reversal if a comparison with the theoretical results in Fig. 4 is to be meaningful. In a following section we consider temperature and composition effects in detail and show that only when these effects are taken into account may theory and experiment for Co, Cu, and Pd be completely reconciled.

### B. Rectangular state-density model

One important conclusion one may draw from the total energy calculations is that the site substitution behavior of ternary additions to  $\text{Ni}_3\text{Al}$  is almost entirely governed by the electronic structure of the added species as originally suggested by Guard and Westbrook.<sup>1</sup> To substantiate this claim we will here explore a simple model based on nearest-neighbor pair interactions which leads to an almost quantitative description of the trends found in Fig. 4.

The first step is to notice that the transfer energy  $E_{\text{Ni} \rightarrow \text{Al}}^X$  at 0 K may be obtained in the dilute limit  $(\eta_{\text{Ni}}, \eta_{\text{Al}}) \rightarrow (1, 1)$  from Eq. (9) and Eq. (A18) in the form

$$E_{\text{Ni} \rightarrow \text{Al}}^X = 4V_{\text{NiXAl}} = 4v_{\text{NiX}} - 4v_{\text{AlX}} + 4v_{\text{AlAl}} - 4v_{\text{NiAl}}, \quad (16)$$

where  $V_{\text{NiXAl}}$  and  $v_{ij}$  are the generalized nearest-neighbor effective pair interactions and interatomic pair potentials defined in Appendix A. The physical interpretation of the last equation is straightforward. In an Al site an X atom has 12 Ni atoms as its nearest neighbors while in a Ni site it has 8 Ni atoms and 4 Al atoms as its nearest neighbors. To move an X atom from a Ni site to an Al site one must therefore break four X-Al bonds and create instead four X-Ni bonds as reflected in the first two terms. The last two terms in Eq. (16) correspond to the energy of the complementary process of moving an Al atom from the Al to the Ni sublattice and this is the same for all X. Therefore, the trends in Fig. 4 is determined only by the competition between the two interatomic pair potentials  $v_{\text{NiX}}$  and  $v_{\text{AlX}}$ .

The variation of the first of these pair potentials,  $v_{\text{NiX}}$ , across a transition series may be obtained in a rectangular  $d$  state density model which is the analogue of Friedel's model for metallic cohesion.<sup>21</sup> If we identify the bonding energy with the sum of nearest neighbor pair potentials we find

$$v_{\text{NiX}} = \frac{1}{6} \frac{1}{20} \bar{n} (10 - \bar{n}) \bar{W}, \quad (17)$$

where the prefactor 1/6 accounts for the 12 nearest neighbors of the fcc lattice. Further,  $\bar{n} = 1/2(n_{\text{Ni}} + n_{\text{X}})$  is the average



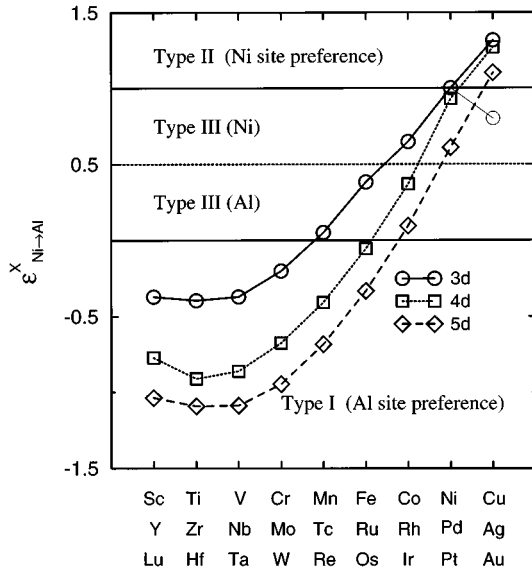


FIG. 5. Estimate of the transfer energy based on the Friedel-like model for Ni-X interactions (17) in the assumption that  $v_{XAl} = v_{NiAl} : \epsilon_{Ni \rightarrow Al}^X = 4(v_{NiX} - v_{NiNi})/E_{ant} + 1$ . The energy of antisite defect formation  $E_{ant}^X \approx 2.00$  eV is taken from the results of the first-principles calculations. Thin open circle is the transfer energy for Cu if one takes into account the fact that  $v_{NiAl} - v_{CuAl} \approx 0.25$  eV.

number of  $d$  electrons per Ni-X bond, and  $\bar{W}$  is the average  $d$ -band width which may be expressed as the geometric mean

$$\bar{W} = \sqrt{W_{Ni} W_X} \quad (18)$$

of the individual bandwidths,  $W_{Ni}$  and  $W_X$ .

To further simplify the model we assume that variation of the second pair potential as a function of  $X$  is small compared to that of  $v_{NiX}$  and that  $v_{AlX}$  may therefore be approximated by  $v_{NiAl}$ . This we will justify below. If we finally note that the energy of forming an antisite defect may be written

$$E_{ant} = 4(v_{AlAl} + v_{NiNi} - 2v_{NiAl}), \quad (19)$$

we find the approximate expression

$$\epsilon_{Ni \rightarrow Al}^X = 4(v_{NiX} - v_{NiNi})/E_{ant} + 1 \quad (20)$$

for the transfer energy. The antisite energy in  $Ni_3Al$  is approximately 2 eV as seen in Fig. 3, and the variation of the site substitution behavior in  $Ni_3Al$  is now entirely governed by the electronic properties in the form of  $d$ -band width and  $d$ -occupation number of the added species.

The approximate transfer energy  $\epsilon_{Ni \rightarrow Al}^X$  has been calculated across the three transition metal series from the  $d$ -band widths and occupation numbers for the pure elements given by Andersen *et al.*<sup>27</sup> and the results are presented in Fig. 5. If we compare these approximate values with those in Fig. 4 we find the same trend and even quantitative agreement except for the noble metals. This means that the site preference for transition metals almost exclusively is determined by the Ni-transition-metal interactions which in turn depend on the average  $d$ -band width and occupation number. This immediately explains the increasing Al site preference for transition metals as one moves from the end to the be-

ginning of a series as the consequence of the decrease in the average  $d$ -band filling. It also explains the increasing Al site preference as one moves down a column of the Periodic Table as a consequence of the well-known increase in  $d$ -band width with the main quantum number.

We now return to the pair potentials,  $v_{XAl}$ , the variation of which we have neglected so far. Unfortunately, it has been demonstrated that these terms cannot be described in a simple form similar to Eq. (17).<sup>36-38</sup> We may, however, use the result of the systematic study by Carlsson<sup>25</sup> of Al-transition-metal interactions. Although he calculated only the effective pair interactions of Al with 3d and 4d metals,  $\tilde{V}_{XAl}$ , the variation of the corresponding pair potentials  $v_{XAl}$  may be deduced from the following relation [see Eq. (A3) in Appendix A]:

$$v_{XAl} = \frac{1}{2} (-\tilde{V}_{XAl} + v_{XX} + v_{AlAl}). \quad (21)$$

Since  $v_{AlAl}$  is independent of  $X$  the only difference between  $\tilde{V}_{XAl}$  and  $v_{XAl}$  is the interatomic pair potential  $v_{XX}$ . If we use the Friedel model (17) with the appropriate parameters  $\bar{W}$  and  $\bar{n}$  we find that  $v_{XX}$  will exhibit the well-known parabolic behavior, i.e.,  $v_{XX}$  will reach its minimum value in the middle of each transition series.<sup>39</sup> Exactly the same trend is found for  $V_{XAl}$  by Carlsson<sup>25</sup> (see also, Ref. 39) and as a result the variation of  $V_{XAl}$  and  $v_{XX}$  in Eq. (21) cancel to a large degree. Hence, relative to  $v_{XNi}$  the variation of  $v_{XAl}$  with  $X$  may be neglected and the assumption that  $v_{XAl} \approx v_{NiAl}$  is a reasonable one for transition metals.

Carlsson<sup>25</sup> also found that Al-noble-metal interactions are significantly smaller than Al-transition-metal interactions. For instance,  $\tilde{V}_{NiAl} - \tilde{V}_{CuAl} \approx 0.5$  eV. One also expects that Ni-Ni interactions are stronger than Cu-Cu interaction, i.e.,  $v_{NiNi}$  is smaller than  $v_{CuCu}$  and thus from Eq. (21)  $v_{NiAl} - v_{CuAl}$  should be at least  $-0.25$  eV. If we use this estimate for  $v_{CuAl}$  instead of  $v_{CuAl} \approx v_{NiAl}$  the value of  $\epsilon_{Ni \rightarrow Al}^{Cu}$  in Fig. 5 is reduced to approximately 0.8 which corresponds to type III(Ni) site preference as obtained in the total energy calculations. Thus the reduction of the Ni site preference for the noble metals is a consequence of their reduced interaction with Al relative to that of the transition metals.

### C. Composition effects

The results presented in the previous section lead to a unified picture of site substitution behavior of ternary additions. The picture is, however, only valid at 0 K and in the dilute limit and may not hold under different conditions. In fact, we will now show that depending on composition and temperature one may find site substitution behavior which is seemingly in contradiction to the classification given in Fig. 4. In particular, we will show that elements belonging to type I may be found on the Ni sublattice at equilibrium, i.e., exhibit type III substitution behavior, and that elements belonging to type III may behave like elements of type I or II.

The site substitution behavior of ternary additions to  $Ni_3Al$  is conventionally discussed in terms of the fraction of  $X$  atoms on the Al sublattice as defined in Sec. II

TABLE I. The ideal value of the fraction  $f$  of  $X$  atoms in the Al sites in different alloy systems.

Site preference	Al deficient $\bar{c}_{\text{Ni}} = 0.75$	Equideficient $\bar{c}_{\text{Ni}}/\bar{c}_{\text{Al}} = 3$	Ni deficient $\bar{c}_{\text{Al}} = 0.25$
I: Strong Al	$f = 1$	$f = 1$	$f = 1$
III: Weak Ni or Al	$f = 1$	$f = 0.25$	$f = 0$
II: Strong Ni	$f = 0$	$f = 0$	$f = 0$

$$f = \frac{c_X(\text{Al})}{c_X(\text{Al}) + 3c_X(\text{Ni})}, \quad (22)$$

from which we immediately deduce a number of simple rules. First, in the completely random state where all concentrations are equal  $f = f_{\text{rand}} = 0.25$ . Second, if all  $X$  atoms are on the Al sites  $f = 1$  and if all  $X$  atom are on the Ni sites  $f = 0$  which are therefore the two values one expects to find at 0 K independent of the alloy composition when the addition  $X$  exhibits either strong Al or Ni site preference. On the other hand, if the  $X$  element exhibits type III substitution behavior  $f$  may take on any value at 0 K, depending on alloy composition, and in particular on the  $\bar{c}_{\text{Ni}}/\bar{c}_{\text{Al}}$  ratio (8). For instance, in the cases of equideficient compositions ( $\bar{c}_{\text{Ni}}/\bar{c}_{\text{Al}} = 3$ ; see Sec. II) where the  $X$  element exhibits very weak site preference, i.e.,  $\tilde{E}_{\text{Ni} \rightarrow \text{Al}}^X \approx 0.5$ ,  $f$  should be equal to 0.25, while in Ni-deficient ( $\bar{c}_{\text{Al}} = 0.25$ ) or Al-deficient ( $\bar{c}_{\text{Ni}} = 0.75$ ) alloys all  $X$  should go either to the Ni or the Al sublattices, i.e.,  $f = 0$  or 1, respectively.

The expected correspondence between alloy composition and the fraction  $f$  at 0 K is summarized in Table I. It is this correspondence which is conventionally used to deduce site preference of a particular addition  $X$  once the  $f$  is known experimentally. Unfortunately, the idealized picture of site substitution behavior at 0 K which is the basis of the table does not hold in all cases if the concentration of the ternary addition increases from the dilute value as we shall now show.

To discuss temperature and composition effects we minimize the free ordering energy

$$F_{\text{ord}}^X(\eta_{\text{Ni}}, \eta_{\text{Al}}) = E_{\text{ord}}^X(\eta_{\text{Ni}}, \eta_{\text{Al}}) - TS, \quad (23)$$

with respect to the LRO parameters. This leads to the Gorsky-Bragg-Williams equations

$$F_{B \rightarrow A}^X(\eta_A, \eta_B) = -\frac{1}{\xi_A \xi_B} \partial F_{\text{ord}}^X / \partial \eta_A = 0, \quad (24)$$

$$F_{A \rightarrow B}^X(\eta_A, \eta_B) = -\frac{1}{\xi_A \xi_B} \partial F_{\text{ord}}^X / \partial \eta_B = 0,$$

for the equilibrium LRO parameters which at 0 K reduce to Eq. (9). To evaluate Eq. (23) the entropy term is calculated in the single-site mean-field approximation

$$S = -k_B \sum_{i\alpha} \xi_{\alpha} c_i(\alpha) \ln[c_i(\alpha)] \quad (25)$$

and the ordering energy  $E_{\text{ord}}^X(\eta_{\text{Ni}}, \eta_{\text{Al}})$  is obtained from Eq. (14) where we assume that the coefficients  $U$  are independent of the alloy composition. Hence the results should be

considered as a qualitative estimate of the effects of composition and temperature on site substitution behavior.

As a first example we show in Fig. 6 the calculated fraction  $f$  for two elements, Cr and Re, which according to Fig. 4 are type I elements, i.e., they exhibit strong Al site preference. If we now apply the simple rules of Table I to these alloys for three compositions, i.e., Al deficient, equideficient, and Ni deficient, we find that the fraction of  $X$  in the Al sites in all cases should be equal to 1 which is most certainly not obeyed by the results in Fig. 6. In fact, only the Al-deficient alloys exhibit the ideal behavior. Moreover, at 0 K the fraction of Cr atoms in the Al sites for the equideficient and Ni-deficient alloys is quite close to the value 0.25, which corresponds to an equal distribution of Cr atoms between the sublattices. If such a fraction had been found in an experiment for an equideficient alloy Cr would according to Table I immediately have been classified as a type III element in

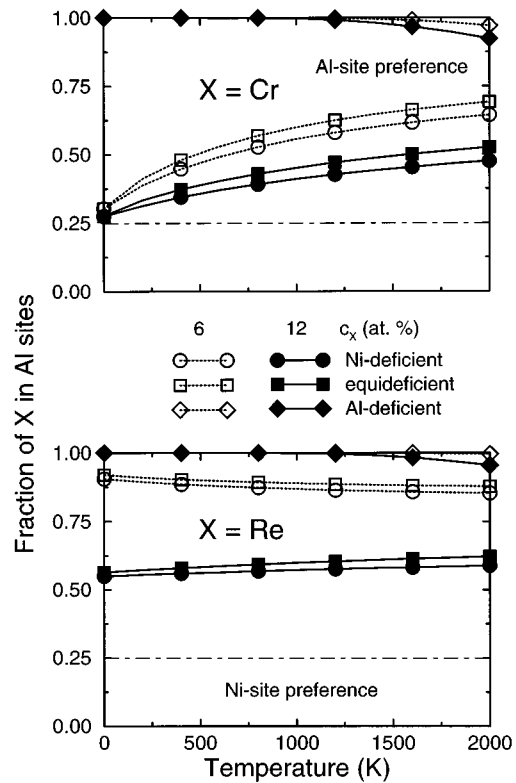


FIG. 6. Cr and Re occupation fraction of Al sites in the Ni-deficient, equideficient, and Al-deficient  $\text{Ni}_3\text{Al}$ . Full lines with filled circles, squares and diamonds correspond to the ternary alloys with  $\bar{c}_X = 12$  at. %:  $\text{Ni}_{63}\text{Al}_{25}\text{X}_{12}$ ,  $\text{Ni}_{66}\text{Al}_{22}\text{X}_{12}$ , and  $\text{Ni}_{75}\text{Al}_{13}\text{X}_{12}$ , and dotted lines with open circles, squares and diamonds correspond to the ternary alloys with 6 at. % of  $X$  element:  $\text{Ni}_{69}\text{Al}_{25}\text{X}_6$ ,  $\text{Ni}_{70.5}\text{Al}_{23.5}\text{X}_6$ , and  $\text{Ni}_{75}\text{Al}_{19}\text{X}_6$ .

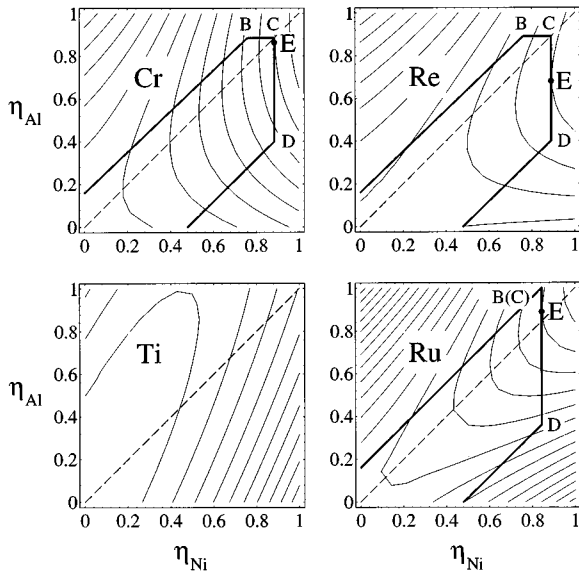


FIG. 7. Contour plot of the ordering energy  $E_{\text{ord}}^X(\eta_{\text{Ni}}, \eta_{\text{Al}})$  for Cr, Re, Ti, and Ru. Point E on the segments of maximally ordered states is the equilibrium point of the system for the corresponding alloy compositions (see text).

contradiction to the theoretical classification. One may argue that Cr is in fact very close to a type III behavior since  $\bar{E}_{\text{Ni} \rightarrow \text{Al}}^{\text{Cr}} = -0.016$ . However, for Re  $\bar{E}_{\text{Ni} \rightarrow \text{Al}}^{\text{Re}} = -0.474$ , and one still finds a fraction of Re in the Al sites which decreases with increasing Re concentration in the cases of Ni-deficient and equideficient alloys to the extent that at 12 at. % it is close to 0.5. Again the simple interpretation of an experiment would lead to an incorrect classification.

To explain the results in Fig. 6 we rewrite the transfer energy  $E_{\text{Ni} \rightarrow \text{Al}}^X$  with the help of the parametrization (14) of the ordering energy

$$E_{\text{Ni} \rightarrow \text{Al}}^X(\eta_{\text{Ni}}, \eta_{\text{Al}}) = -\frac{32}{3}(U_{\text{Al-X}}\eta_{\text{Al}} - U_{\text{Ni-Al-X}}\eta_{\text{Ni}}). \quad (26)$$

In the dilute limit and at 0 K the segments of the maximally ordered state in the LRO space become infinitesimal and thus one may safely assume that  $E_{\text{Ni} \rightarrow \text{Al}}^X$  has the same value in all points of the maximally ordered state, i.e.,  $E_{\text{Ni} \rightarrow \text{Al}}^X(B) \approx E_{\text{Ni} \rightarrow \text{Al}}^X(C) \approx E_{\text{Ni} \rightarrow \text{Al}}^X(D) \approx E_{\text{Ni} \rightarrow \text{Al}}^X(1,1)$ . However, when the concentration of the ternary addition is sufficiently large one must consider the possibility of changing the relative contributions of  $U_{\text{Al-X}}$  and  $U_{\text{Ni-Al-X}}$  to  $E_{\text{Ni} \rightarrow \text{Al}}^X$  in Eq. (26) along the line of maximally ordered states. For instance, in the case of  $\text{Ni}_{66}\text{Al}_{12}\text{X}_{12}$  for type I elements one should consider the points on the line CD in Fig. 7. If point D does not correspond to equilibrium, i.e.,  $E_{\text{Ni} \rightarrow \text{Al}}^X > 0$  in D, the equilibrium order parameters will be somewhere else on the segment CD and may be found by solving the equation  $E_{\text{Ni} \rightarrow \text{Al}}^X = 0$ .<sup>40</sup> In this case a number of X atoms will be also on the Ni sublattice in the equilibrium state, and the fraction of X in the Al sites will be less than 1 ( $f=1$  in point D).

In Fig. 7 we show that this is exactly the case for Cr and Re in the equideficient  $\text{Ni}_{66}\text{Al}_{22}\text{X}_{12}$  alloys. For Cr the point of equilibrium turns out to be (0.89, 0.864), leading to

$f=0.275$ , which is indeed very close to the point C (0.89, 0.89) where the equilibrium point of a type III element is supposed to be. In the case of Re in  $\text{Ni}_{66}\text{Al}_{22}\text{Re}_{12}$  the equilibrium point E is (0.89, 0.679), i.e., practically in the middle of the segment CD and here  $f=0.56$ .

The necessary condition for an element of type I to be only in Al sites at 0 K may be formulated if we assume that the most extreme position of the D point will be on the  $\eta_{\text{Ni}}$  axis corresponding to  $\eta_{\text{Al}}=0$  and that at this point  $E_{\text{Ni} \rightarrow \text{Al}}^X$  must be negative.<sup>41</sup> Hence, in terms of the coefficients of the expansion of the ordering energy (14) we have  $U_{\text{Ni-Al-X}} \leq 0$  or alternatively in terms of the effective pair interactions (A4)

$$\tilde{V}_{\text{NiX}} + \tilde{V}_{\text{AlX}} - \tilde{V}_{\text{NiAl}} \leq 0. \quad (27)$$

In the present calculations the condition is satisfied for the type I elements Sc, Ti, V, Y, Zr, Nb, Mo, Lu, Hf, Ta, and W but not for Cr, Tc, Re, and Os. So, the latter elements may substitute for Ni at some ternary alloy compositions even in the case where the alloy is not Ni deficient. It is also worth mentioning that the condition (27) is automatically satisfied for type I elements if the contours of constant ordering energy are ellipses, i.e.,  $U_{\text{Ni-X}}U_{\text{Al-X}} - U_{\text{Ni-Al-X}}^2 > 0$ . The ordering energy of the Ni-Al-Ti system shown in Fig. 7 is such an example. In this case all the coefficients,  $U_{\text{Ni-X}}$ ,  $U_{\text{Al-X}}$ , and  $U_{\text{Ni-Al-X}}$  should be negative to satisfy the other necessary condition  $E_{\text{ord}}(1,1) = U_{\text{Ni-X}} + U_{\text{Al-X}} - 2U_{\text{Ni-Al-X}} < 0$ . In fact, it is easy to show that if the contours of constant ordering energy are ellipses, the minimum of the ordering energy can be reached only at the ends of the segments of the maximally ordered states, i.e., in the points B, C, or D.

Another example of the violation of the simple rules of Table I can be found in Fig. 8. Here Ru which is classified as type III(Al) is seen to substitute for Al in the Al sublattice at 0 K in the  $\text{Ni}_{69}\text{Al}_{25}\text{Ru}_6$  and  $\text{Ni}_{63}\text{Al}_{25}\text{Ru}_{12}$  alloys in spite of the fact that these are Ni deficient alloys. The origin of this violation is the same as in the two previous cases: The general classification does not work because of the strong dependence of the transfer energy on the values of LRO parameters (26). In Fig. 7 one finds the equilibrium point E for  $\text{Ni}_{63}\text{Al}_{25}\text{Ru}_{12}$  to be (0.84, 0.89) while point C is (0.84, 1.0). As in the case of Cr and Re, the contours of constant ordering energy are hyperbolas,  $U_{\text{Ni-X}}U_{\text{Al-X}} - U_{\text{Ni-Al-X}}^2 < 0$ , and thus E lies between B(C) and D.

Finally, we mention that it is in principle possible to have very sharp site substitution reversal with alloy composition at 0 K for type III element if the constant ordering energy contours are ellipses. In contrast to the type I and type II elements whose equilibrium point should be either B or D of the segment of the maximally ordered states independent of the alloy composition, the equilibrium point of a type III element may at some alloy composition jump from point C, which is the equilibrium point in the dilute limit, to points B or D depending on the site preference of the element.

#### D. Temperature effects

If the composition dependence of the site occupation is somewhat unexpected so is the temperature dependence seen in Fig. 6, in particular in the case of Cr. In a completely random alloy the fraction of X, Ni, and Al in the Al sites

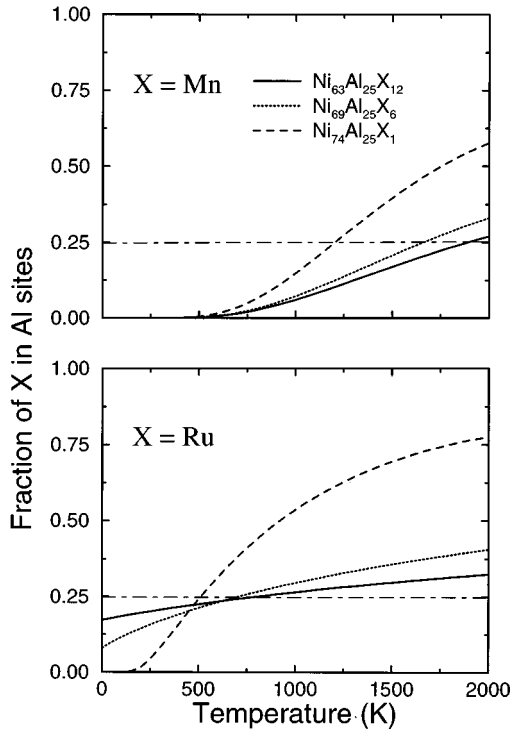


FIG. 8. Mn (upper panel) and Ru (lower panel) occupation fraction of Al sites in Ni-deficient alloys. Full lines are the result for  $\text{Ni}_{63}\text{Al}_{25}\text{X}_{12}$ , dotted lines for  $\text{Ni}_{69}\text{Al}_{25}\text{X}_6$ , and dot-dashed lines for  $\text{Ni}_{74}\text{Al}_{25}\text{X}_1$ .

should be equal to 0.25, i.e., as one approaches the order-disorder transition temperature all the curves in the figure should converge towards this value. In other words, taking into account the fact that the entropy contribution to the free energy increases with temperature and gives rise to an increasing randomness in the system, one may expect that the fraction of the elements on the Al sublattice will change monotonically from its value at 0 K to 0.25 at the order-disorder transition temperature. In fact, exactly the opposite dependence is found for Cr, where for Ni-deficient and equideficient compositions the fraction of Cr in the Al sites increases with temperature. It is easy to see that if  $E_{\text{Ni} \rightarrow \text{Al}}^{\text{Cr}}$  had been slightly positive rather than slightly negative the fraction of Cr atoms in the Al sites would be 0 at low temperature for the same Ni-deficient alloys and that one may therefore observe a site occupation reversal with increasing temperature. In Fig. 8 we show further examples of this effect for Mn and Ru.

The possibility of a reversal of the site preference with temperature was first discussed by Wu *et al.*<sup>14</sup> in their model calculations of site occupation by means of the cluster variation method (CVM). The results of this study appear to have been overlooked, possibly because the authors concluded that “the change in site occupation with temperature is generally small.” Here, we shall show that such a change may indeed be quite pronounced and we shall give a physically simple picture of the phenomenon.

Before we proceed, we would like to emphasize that as both the ordering energy and the entropy are nonlinear functions of the order parameters, see Fig. 7 and Fig. 9, one may expect temperature to lead to a very complex behavior in the

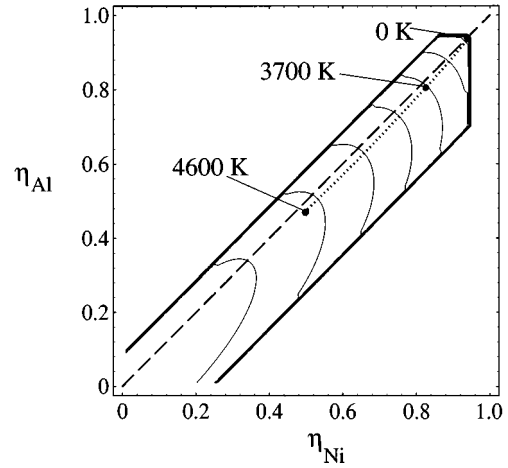


FIG. 9. Contour plot of the mean-field entropy (25) for  $\text{Ni}_{70.5}\text{Al}_{23.5}\text{X}_6$ . The dashed line corresponds to  $\eta_{\text{Ni}} = \eta_{\text{Al}}$ . The dotted line is the trajectory of the  $\text{Ni}_{70.5}\text{Al}_{23.5}\text{Fe}_6$  alloy with the temperature.

LRO space of ternary systems. This is in contrast to binary alloys which only have the possibility to move along the line  $\eta_A = \eta_B$ , Fig. 1, creating or annihilating exchange antisite defects. In the case of ternary alloys, on the other hand, new types of defects may be created allowing the system the possibility to move in any direction in LRO space. Seen in this light the phenomenon of site occupation reversal may not be so unexpected since it simply corresponds to the crossing of the line  $\eta_A = \eta_B$  in the LRO space by the equilibrium point.

To arrive at a necessary condition for a system to undergo site substitution reversal with temperature let us consider the energetics of site distribution of a Ni-deficient alloy with a small amount of Ru. Now, Ru is classified as a type III(Al) metal which means that it prefers Al sites but cannot move from a Ni site to an Al site at the cost of forming an antisite defect. In the Ni deficient alloy at 0 K all the Ru atoms must therefore reside on the Ni sublattices, i.e., the atomic fraction of Ru in Al sites should be zero (see Fig. 8). In this case the Al sublattice is “pure.” When the temperature increases the entropy term makes the existence of such a “pure” sublattice energetically unfavorable. Thus both Ni and Ru atoms may go from the Ni sublattices to the Al sublattice and create substitutional defects.

The energy of moving a Ni atom from the Ni sublattices to the Al sublattice is the energy of forming an exchange antisite defect  $E_{\text{Ni} \rightarrow \text{Al}}^{\text{Ni}} = E_{\text{ant}}^{\text{xc}} \sim 2.0$  eV while the energy of moving a Ru is  $E_{\text{Ni} \rightarrow \text{Al}}^{\text{Ru}}$  which is only 0.25 eV; see Fig. 3. In the limit  $T \rightarrow 0$  the concentration of both defects is proportional to  $\exp(-E_{\text{Ni} \rightarrow \text{Al}}^{\text{X}}/2kT)$  and at temperatures well below the order-disorder transition temperature it is therefore preferentially Ru atoms which move from the Ni to the Al sublattice. The question is how far this transfer of Ru atoms from the Ni to the Al sublattice will go at a given temperature before equilibrium is reached. To answer this one must consider the compensating process of transferring Ru atoms from the Al to the Ni sublattice.

The energy of moving a Ru from the Ni sites to Al sites  $E_{\text{Al} \rightarrow \text{Ni}}^{\text{Ru}} = E_{\text{ant}}^{\text{xc}} - E_{\text{Ni} \rightarrow \text{Al}}^{\text{Ru}} = 1.75$  eV which is much higher than  $E_{\text{Ni} \rightarrow \text{Al}}^{\text{Ru}}$  but still less than the energy of forming the exchange

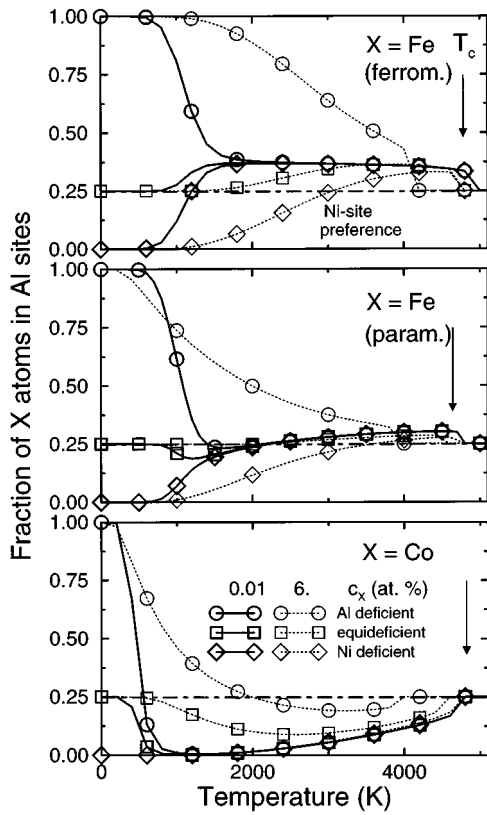


FIG. 10. Site occupation of ferromagnetic Fe (upper panel), paramagnetic Fe (middle panel), and Co (lower panel) in the Ni-deficient, equideficient, and Al-deficient  $\text{Ni}_3\text{Al}$ .  $T_c$  is the order-disorder transition temperature.

antisite defect. Therefore, the thermally most activated process in the system will always be the transfer of Ru atoms from the Ni to the Al sublattice, and thus at some temperature below the order-disorder transition temperature the Ru atoms will be equally distributed among the sublattices. At this point the fraction  $f$  of Ru atoms in the Al sites is 0.25. If we increase the temperature further more Ru atoms will transfer to the Al sublattice thereby increasing  $f$ . This effect will be seen as a site substitution reversal. Hence the necessary condition for an  $X$  element to exhibit a temperature driven site substitution reversal in an  $A$ -deficient ordered  $AB(X)$  alloy may be written as

$$0 < E_{A \rightarrow B}^X < \frac{1}{2} E_{\text{ant}}^{\text{xc}}. \quad (28)$$

It may seem that Eq. (28) will be correct only in the case of equiatomic binary ordered alloys where the number of  $A$  sublattices is equal to the number of  $B$  sublattices. For instance, it follows from Eq. (28) that if  $E_{A \rightarrow B}^X = E_{B \rightarrow A}^X = 1/2 E_{\text{ant}}^{\text{xc}}$  i.e., element  $X$  does not exhibit any site preference, then there will be no site substitution reversal with temperature. According to Fig. 4 ferromagnetic Fe has essentially no site preference. However, as one may see in Fig. 10 there is a site substitution reversal for Ni deficient alloys which looks like weak Al site preference for ferromagnetic Fe. Moreover, paramagnetic Fe, which has weak Ni site pref-

erence, i.e., type III(Ni), also exhibits site substitution reversal for Ni deficient alloys but not for Al-deficient in apparent violation of Eq. (28).

To explain the origin of this kind of site substitution reversal we note that  $E_{A \rightarrow B}^X / E_{B \rightarrow A}^X = \text{const}$  along the line  $\eta_A = \eta_B$  in the LRO space if the ordering energy has the quadratic form (14). This means that in the dilute limit of  $X$  where the system must be in the infinitesimal vicinity of this line, the ordering energy plays no role in the site reversal found for Fe. Therefore, the site substitution reversal of ferromagnetic as well as paramagnetic Fe in Ni deficient alloys must be a purely entropic effect.

At first sight this conclusion seems to be inconsistent with the statistical nature of the entropy which is responsible only for braking the order in the system. Nevertheless, it can easily be shown that the entropy does in fact increase the Al site preference for all ternary additions to  $\text{Ni}_3\text{Al}$  including Fe. Let us consider a dilute alloy of ferromagnetic Fe in equideficient  $\text{Ni}_3\text{Al}$ . At 0 K all the Fe atoms are distributed equally between sublattices, i.e., the system is in point  $C$  exactly on the line  $\eta_{\text{Ni}} = \eta_{\text{Al}}$  ( $f = 0.25$ ). When we increase the temperature the system will move along the direction of the gradient field of the free ordering energy in LRO space, i.e., in the direction given by  $-\nabla F_{\text{ord}} = -\nabla E_{\text{ord}} + T \nabla S$ .

The gradient of the ordering energy (14) is

$$-\nabla E_{\text{ord}} = \xi_A \xi_B (E_{A \rightarrow B}^X \hat{\eta}_A + E_{B \rightarrow A}^X \hat{\eta}_B), \quad (29)$$

which for ferromagnetic Fe where  $E_{\text{Ni} \rightarrow \text{Al}}^{\text{Fe}} = E_{\text{Al} \rightarrow \text{Ni}}^{\text{Fe}}$  points along (1,1) in the direction of larger LRO parameters. Thus, the ordering energy cannot lead to deviations from the line  $\eta_{\text{Ni}} = \eta_{\text{Al}}$  and thereby transfer Fe atoms from one sublattice to the other.

The gradient of the entropy may be given by

$$\begin{aligned} \nabla S = & -k_B \xi_A \xi_B \left( \ln \frac{1 - \bar{c}_X + (m/k) \eta}{1 - \bar{c}_X - \eta} \hat{\eta}_A \right. \\ & \left. + \ln \frac{1 - \bar{c}_X + (k/m) \eta}{1 - \bar{c}_X - \eta} \hat{\eta}_B \right), \end{aligned} \quad (30)$$

where we have used the single site mean field approximation (25) for an equideficient ternary  $A_k B_m$  alloy with equal distribution of  $X$  atoms between sublattices, i.e.,  $\eta_A = \eta_B = \eta$ . In the case of  $\text{Ni}_3\text{Al}$  this may be written

$$\nabla S = -k_B \frac{3}{16} \left( \ln \frac{1 - \bar{c}_X + 1/3 \eta}{1 - \bar{c}_X - \eta} \hat{\eta}_{\text{Ni}} + \ln \frac{1 - \bar{c}_X + 3 \eta}{1 - \bar{c}_X - \eta} \hat{\eta}_{\text{Al}} \right). \quad (31)$$

It follows from Eq. (30) that in an equiatomic, ordered alloy where the number of  $A$  and  $B$  sublattices are the same, i.e.,  $k = m$ , the entropy gradient field on the line  $\eta_A = \eta_B$  points along (1,1) and therefore cannot make the system move away from this line. For  $\text{Ni}_3\text{Al}$ , however, Eq. (31) shows that due to the fact that  $k \neq m$  the  $\eta_{\text{Al}}$  component of the gradient is larger than the  $\eta_{\text{Ni}}$  component. Since the entropy gradient points in the direction of lower LRO parameters, i.e., opposite to the gradient of the ordering energy, one finds that with increasing temperature the system will move away from  $\eta_{\text{Ni}} = \eta_{\text{Al}}$  into the region  $\eta_{\text{Ni}} > \eta_{\text{Al}}$  thereby increasing the number of Fe atoms in the Al sites and  $f$ .

An asymmetrical form of the entropy is seen in Fig. 9 where the isoentropic lobes are aligned along  $\eta_{\text{Ni}} = \eta_{\text{Al}}$  but slightly shifted towards greater values of  $\eta_{\text{Ni}}$ . Hence, if a ternary addition to  $\text{Ni}_3\text{Al}$  does not have any site preference, the system will with increasing temperature move away the line  $\eta_{\text{Ni}} = \eta_{\text{Al}}$  into the region  $\eta_{\text{Ni}} > \eta_{\text{Al}}$ . The effect is demonstrated in the figure by the trajectory of equideficient  $\text{Ni}_3\text{Al}$  with 6 at. % of ferromagnetic Fe. At 0 K the system is on the line  $\eta_{\text{Ni}} = \eta_{\text{Al}}$ , but with increasing temperature it starts to move to the greater values of  $\eta_{\text{Ni}}$ . At 3700 K the difference between  $\eta_{\text{Ni}}$  and  $\eta_{\text{Al}}$  reaches the value of 0.036 and remains almost constant up to the temperature of order-disorder transition, 4600 K. Therefore, the fraction of Fe in the Al sites in this alloy is practically constant (see Sec. II) between 3700 and 4600 K. This effect is clearly seen in Fig. 10 and it becomes much more pronounced in the dilute limit,  $\bar{c}_{\text{Fe}} = 0.01$  at. %. Here the fraction of Fe atoms in the Al sites becomes constant ( $f \approx 0.36$ ) at a much lower temperature, 2000 K and not only for the equideficient but also for the Ni and Al deficient alloys.

Such an entropy induced site preference may lead to unusual, nonmonotonic site occupation behavior with temperature an example of which is clearly seen in Fig. 10 for a dilute solution ( $\bar{c}_X = 0.01$  at. %) of the paramagnetic Fe in the equideficient alloy. At approximately 1000 K the fraction of Fe atoms in the Al sites drops slightly, i.e.,  $f$  becomes smaller than 0.25, and then at 1500 K the fraction of Fe in Al site begins to increase, so that at 2300 K  $f$  is already greater than 0.25. The reason for such a double site substitution reversal is the following. At low temperatures the ordering energy contribution to the ordering free energy is dominating the system, i.e., the movement of the system in LRO space is basically determined by  $\nabla E_{\text{ord}}$ , Eq. (29). Therefore, paramagnetic Fe having a weak Ni site preference moves from the Al to Ni sublattices. With increasing temperature, however, the contribution of the entropy to the free ordering energy increases relative to that of the ordering energy. Therefore, at some temperature the movement of the system will be determined by  $\nabla S$  and the transfer of Fe atoms changes direction, i.e., they start to move from the Ni to Al sublattice. If the order-disorder transition temperature is sufficiently high the system again undergoes a site substitution reversal transition, exhibiting Al site preference.

It is worth mentioning that such a nonmonotonic site occupancy is in fact connected with an asymmetrical form of the entropy, but not with the number of alloy components. This means that it may also be observed in the case of complex binary ordered alloys if the number of A- and B-type of sublattices is greater than two and the number of different A or B sublattices is also different. For instance, the temperature driven site substitution reversal in the binary Fe-Cr  $\sigma$  phase recently found by Sluiter *et al.*<sup>42</sup> is most probably caused by the entropy induced site preference rather than by "the competition between single site interactions and multi-site interactions." In fact the results in their Fig. 4 for the "C site" are qualitatively very similar to the results for paramagnetic Fe in equideficient alloys discussed above in the sense that first the fraction of Fe atoms in the C sites drops slightly and then it increases monotonically above its initial value at 0 K.

Finally, we would like to point out that the smaller the concentration of the ternary addition the more pronounced the site substitution reversal will be, and that in the dilute limit of the ternary addition the transition may be very sharp. Such is the case for Co in the Al deficient alloy,  $\text{Ni}_{75}\text{Al}_{24.99}\text{Co}_{0.01}$ , shown in Fig. 10 where the fraction of Co atoms in the Al sites drops to practically zero at 1200 K. The subsequent increase in the fraction with temperature is again a consequence of the increasing entropy-induced Al site preference. However, in contrast to paramagnetic Fe the second site occupation reversal transition does not occur in this case since the preference of Co atoms for the Ni sites is much stronger than that of paramagnetic Fe.

### E. Cu and Pd in Al-deficient alloys

At this point it should be clear that unless one has complete control over composition and temperature effects it may not be particularly meaningful to compare theory and experiment as far as site occupation of ternary additions to  $\text{Ni}_3\text{Al}$  is concerned. In fact by doing so one may reach incorrect conclusions. For instance, it is generally believed that ternary phase diagrams, see, e.g., Refs. 12 and 18 which discuss most of the experimental work, lead to reliable information concerning site preferences in spite of the model calculations by Wu *et al.*<sup>14</sup> which demonstrate that at finite temperatures the site preference of the ternary addition may in generally not be related to the direction of the solubility lobe of the ordering phase. In the next section we shall show that this result of Wu *et al.*<sup>14</sup> in fact holds also at 0 K. Further, as one may realize from the previous section the site substitution behavior may be very sensitive to changes in both composition and temperature. It is therefore practically impossible to analyze the experimental work on many component alloys; see, e.g., Ref. 43, in terms of the site occupation behavior of the added species. Finally, it is also practically impossible for us to discuss experimental results which contradict each other.<sup>8,10,11</sup> We may however, discuss two recent experimental investigations<sup>6,7</sup> the results of which are accepted as conclusive evidence for the classification of Cu and Pd are type II elements.

The simplest way to distinguish whether an X element exhibits type II or type III(Ni) substitution behavior is to find its fraction in the Al sites (or Ni sites) of Al deficient alloys, as one can see from Table I. If all the X atoms are on the Ni sublattices, i.e., the fraction of X atoms in the Al sites is zero, then X is a type II element. Experiments of this kind have been performed by Chiba *et al.*<sup>6</sup> for Pd by means of the atom location by channeling microanalysis (ALCHEMI) technique and for Cu by Hono *et al.*<sup>7</sup> by means of atom probe field ion microscopy (APFIM). In both experiments the ternary alloy composition was  $\text{Ni}_{75}\text{Al}_{23}\text{X}_2$  and in both experiments it was found that Cu and Pd occupy almost exclusively the Ni sublattice. However, even though the measurements were performed at low temperatures, e.g., for Cu at 30 K, the samples were in fact annealed at approximately 1300 K,  $\text{Ni}_{75}\text{Al}_{23}\text{Cu}_2$  for 24 hours and  $\text{Ni}_{75}\text{Al}_{23}\text{Pd}_2$  for 5 days, and the latter was quenched in "iced water." Since the diffusion at ambient temperatures is very low it is reasonable to expect that what has in fact been measured in both these experiments is the fraction of Cu and Pd in the Al sites at about

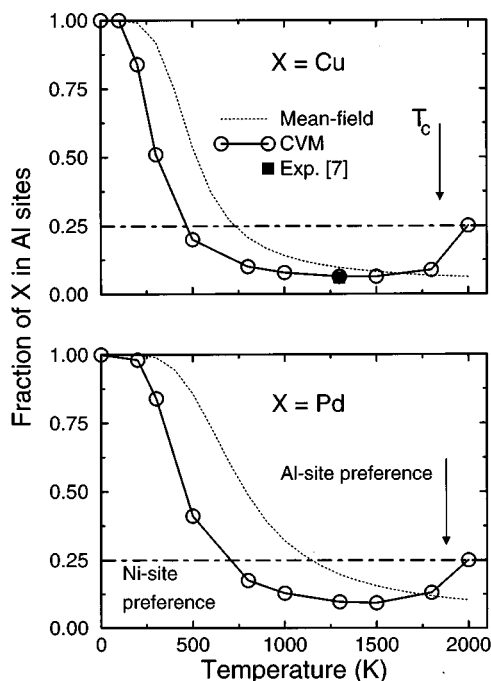


FIG. 11. Site occupation reversal in  $\text{Ni}_{75}\text{Al}_{23}\text{Cu}_2$  and  $\text{Ni}_{75}\text{Al}_{23}\text{Pd}_2$ . Mean-field results (dotted curves) are obtained as in Fig. 10 without any fit of interatomic interactions to the order-disorder transition temperature.

1000–1300 K. Conclusions as to the low temperature behavior of Cu and Pd in  $\text{Ni}_3\text{Al}$  must therefore include considerations of site occupation reversal.

To determine the fraction of Cu and Pd at these temperatures we performed calculations of the fraction of these elements in the Al sites by means of the cluster variation method<sup>44</sup> (CVM) for the entropy, rather than single-site mean-field theory, under the assumption that there are only nearest-neighbor pairwise interactions in the system. The values of these interactions have been obtained from coefficients  $U_{\text{Al-X}}$ ,  $U_{\text{Ni-X}}$ , and  $U_{\text{Ni-Al-X}}$  using their connection with corresponding EPI. To reproduce the experimentally determined order-disorder transition temperature in binary  $\text{Ni}_3\text{Al}$ ,  $\sim 1800$  K,<sup>45</sup> we renormalize the interaction parameters by a factor of 0.75. The reason why the order-disorder transition temperature is usually overestimated in first-principle calculations is not clear, but as pointed out by Carlsson and Sanchez<sup>46</sup> part of the discrepancy is caused by an overestimate of the enthalpy of formation of  $\text{Ni}_3\text{Al}$  in the LDA.

In Fig. 11 we show the calculated fraction of Cu and Pd in the Al sites with the entropy obtained by the CVM. As expected from the fact that both Cu and Pd are classified as type III(Ni) metals, they exhibit site substitution reversal at elevated temperatures similar to the case of Co shown in Fig. 10. Further, the reversal temperature is sufficiently low,  $\sim 400$  K for Cu and  $\sim 600$  K for Pd, that at 1300 K the fraction of Cu in the Al sites of  $\text{Ni}_{75}\text{Al}_{23}\text{Cu}_2$  is 0.07 in excellent agreement with the experimental value of 0.06 (+0.01; -0.06).<sup>7</sup> Similarly, at 1300 K the fraction of Pd in the Al sites of  $\text{Ni}_{75}\text{Al}_{23}\text{Pd}_2$  is calculated to be 0.10 while three measured values range from -0.17 to 0.03 with statistical error of about  $\pm 0.2$ .<sup>6</sup> Thus, none of these experiments

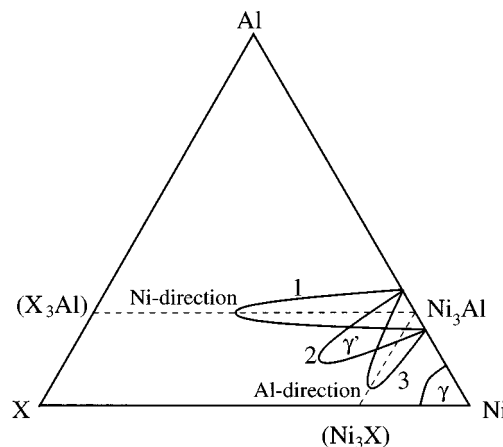


FIG. 12. Schematic presentation of the three different types of the  $\gamma'$  solubility lobes in the ternary Ni-Al-X phase diagrams (1) aligned along the “Al direction” (constant Al concentration), (3) along the “Ni direction” (constant Ni concentration), and (2) intermediate.

may be considered proof of a strong Ni site preference for Cu and Pd, rather they show only the existence of an at least weak Ni site preference.

## VI. ENTHALPY OF FORMATION AND PHASE EQUILIBRIUM BETWEEN $\gamma'$ - AND $\gamma$ - $\text{Ni}_3\text{Al}$ AT 0 K

As has been mentioned above, starting from the work of Guard and Westbrook<sup>1</sup> and up to the present time,<sup>18</sup> the site substitution behavior of most ternary additions to  $\text{Ni}_3\text{Al}$  has been deduced from the direction of the solubility lobe of the  $\gamma'$  phase in the ternary phase diagrams.<sup>12</sup> That is, if the solubility lobe of the  $\gamma'$  phase extends in the direction of constant Ni concentration, i.e., in the “Al direction,” see Fig. 12, the ternary addition should have strong Al site preference. The elements among the transition metals for which this is the case are Ti, Hf, V, Nb, Ta, and Mo which corresponds completely to the theoretical classification in Fig. 4. Similarly, if the solubility lobe extends in the direction of constant Al concentration, i.e., in the “Ni direction,” the corresponding alloying element should exhibit strong Ni-site preference. The elements for which this is the case is Co, Cu, and Pd and Co; see, e.g., Refs. 1, 2, 12, and 47, and these elements are therefore classified experimentally as type II elements in contradiction to the classification in Fig. 4. Finally, if direction of the solubility lobe is intermediate between the two, a type III site substitution behavior is deduced. This is the case for Cr and Fe.

To investigate the relationship between the site preference of a ternary addition and the direction of the solubility lobe Wu *et al.*<sup>14</sup> calculated the phase boundaries between the  $\gamma'$  and  $\gamma$  phases (Ni-based fcc solid solution) in the tetrahedron approximation of the CVM method for some model pair interactions. They found that such a connection does in fact exist if the strength of the pair interaction of a ternary addition with one of the alloy components is much stronger than the interaction with other, i.e., if the ternary addition exhibits strong site preference for one of the sublattices. At the same time, they demonstrated that the direction of the solubility

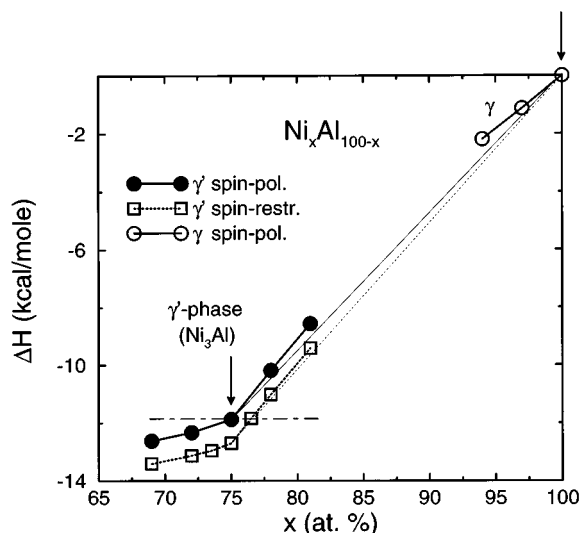


FIG. 13. Enthalpy of formation of binary  $\gamma'$  and  $\gamma$  phases at 0 K as a function of the Ni concentration. The thin line is the common tangent determining the equilibrium  $\gamma'$  and  $\gamma$  compositions in the two-phase Ni-rich alloys at 0 K (shown by arrows). The dashed-dotted line shows the value of the enthalpy of formation of completely ordered  $\text{Ni}_3\text{Al}$ .

lobe may change with temperature if the pair interactions between a ternary addition and either alloy component are similar, i.e., for ternary addition exhibiting weak site preference. As a result, they concluded that the site preference of ternary additions may in general not be related to the direction of the solubility lobe at finite temperatures.

It is the purpose of the present Section to demonstrate that this important result obtained by Wu *et al.*<sup>14</sup> holds also at 0 K. To do so we consider the phase boundaries between  $\gamma'$  and  $\gamma$  Ni-Al and assume that it is the equilibrium between these two phases which is mainly responsible for the direction of the solubility lobe of  $\gamma'$ . We start by investigating the binary system and show in Fig. 13 the calculated enthalpy of formation of  $\gamma'$  Ni-Al. It is seen that the enthalpy is a smooth and almost linear function of the concentration except at the stoichiometric composition where there is a discontinuous change in slope. This discontinuity in slope is connected with the change of the type of partial antisite defects in the alloy, i.e., in the case of a Ni-deficient alloy,  $\bar{c}_{\text{Ni}} < 75$  at. %, there are only Al partial antisite defects on the Ni sublattices, while in the case of Al deficiency there are only Ni partial antisite defects on the Al sublattice (the difference in both slopes is equal to the energy of the exchange antisite defect at stoichiometric composition). Therefore the common tangent which connects the free energy, or here at 0 K the enthalpy of formation, of the  $\gamma'$  and  $\gamma$  phases will touch at 75 and 100 at. %, respectively. In other words, any alloy between 75 and 100 at. % Ni will be phase separated into pure Ni and completely ordered  $\text{Ni}_3\text{Al}$  at 0 K in the absence of any other stable ordered phases in this concentration range. With increasing temperature exchange antisite defects will appear and the free energy will no longer be discontinuous. As a result, the phase boundary between the  $\gamma'$  and the  $\gamma$  phases moves slightly towards greater Ni concentrations although the effect is quite small even 1273 K as may be seen in Fig. 4 of Ref. 46.

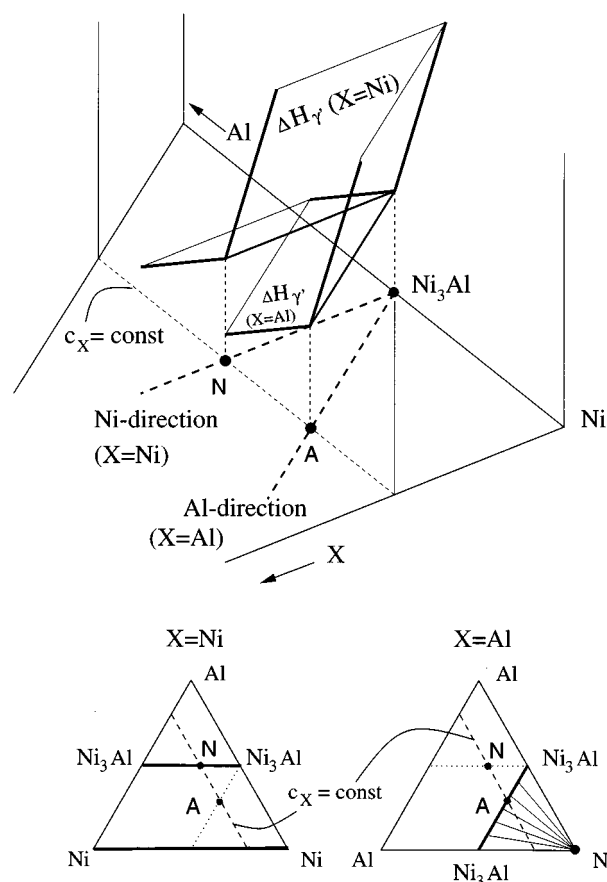


FIG. 14. Schematic presentation of the surfaces of the enthalpies of formation of the  $\gamma'$  phase in the coordinates of the triangle of ternary alloy compositions for  $X = \text{Ni}$  and  $\text{Al}$ . Bold lines correspond to the section of these surfaces by the planes  $\bar{c}_X = 0$  and  $\bar{c}_X = \text{const}$ . The points  $N$  and  $A$  indicate the position of the fold on the line  $\bar{c}_X = \text{const}$ . The corresponding phase diagrams at 0 K for Ni-Al-Ni and Ni-Al-Al systems are shown in the lower part of the figure. Bold lines correspond to  $\text{Ni}_3\text{Al}$  and pure Ni. Thin lines in the Ni-Al-Al phase diagram show tie-lines which in this particular case are generated only by one common-tangent plane. For the Ni-Al-Ni system any line connecting points of the  $\text{Ni}_3\text{Al}$  and Ni phases is the tie-line. The region between the "Ni-direction" and the "Al-direction" constitutes the region of quasistoichiometric alloy compositions.

What is a simple task in a binary system becomes quite time consuming in ternary systems, especially if one wants to consider all 27 ternary additions included in the present work. The reason is that in this case it is necessary to determine the points of contact of common tangent planes, where each plane determines only one point of the phase boundary for each phase, to the free energy surfaces of the two phases obtained in some region of the ternary phase diagram. Fortunately, it turns out that for most ternary additions the boundary of the  $\gamma'$  phase may easily be estimated because the characteristic concentration dependence of the enthalpy of formation of the  $\gamma'$  phase is carried over from the binary system. To clarify our point one may consult Fig. 14 where Ni and Al themselves are taken to be the added element  $X$ . In that case the results presented in Fig. 13 may be considered a section of the surface of the enthalpy of formation along the



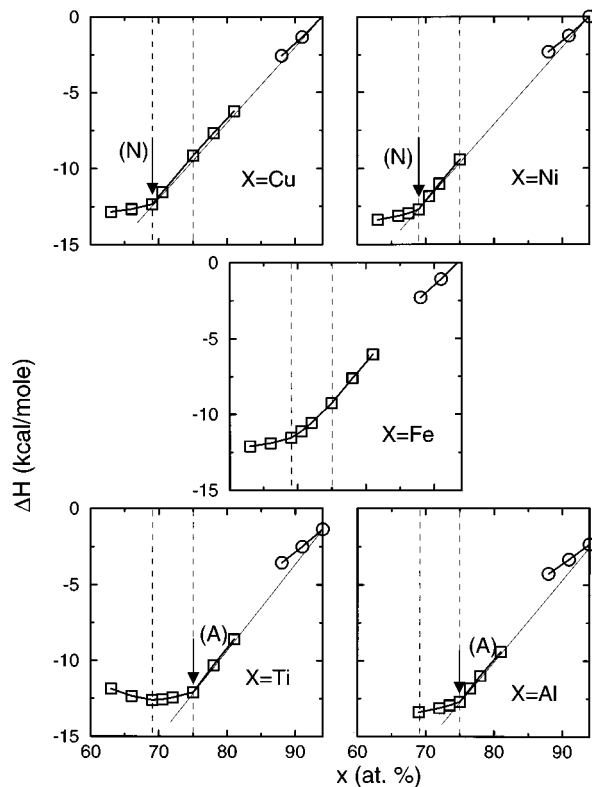


FIG. 15. Enthalpies of formation of ternary partially ordered  $\text{Ni}_x\text{Al}_{94-x}\text{X}_6$  alloys as function of Ni concentration for  $X = \text{Cu}, \text{Ni}, \text{Fe}, \text{Ti},$  and  $\text{Al}$  which are the sections of the enthalpy of formation surfaces along the line  $\bar{c}_X = 6$  at. %. The region of quasistoichiometric compositions are shown by dashed lines. The arrows indicate the position of the fold of the surface of the enthalpy of formation. All the results are obtained for paramagnetic  $\gamma'$ .

line  $\bar{c}_X = 0$  which is the same for all  $X$ . If we now move along a line  $\bar{c}_X = \text{const} \neq 0$  as shown schematically in the upper part of Fig. 14 we find sections of the surfaces of the  $\gamma'$  enthalpies for  $X = \text{Al}$  and  $\text{Ni}$  which are simply rigid shifts of the binary  $\gamma'$  enthalpy along the Ni direction when  $X = \text{Ni}$  and along the Al direction when  $X = \text{Al}$ . As a result the enthalpy surface will have a fold along the Ni direction former case and a fold along the Al direction in the latter case and the corresponding phase diagrams will look as shown in the lower part of Fig. 14.

It follows, that if the surface of the enthalpy of formation has a fold along a line  $\bar{c}_X = \text{const}$  this may indicate a possible direction of the solubility lobe of  $\gamma'$  in the ternary phase diagram of  $\text{Ni-Al-X}$ . This appears to be the case for most transition metals. In Fig. 15 we show such quasibinary sections for  $\text{Cu}, \text{Fe},$  and  $\text{Ti}$ , for  $\bar{c}_X = 6$  at. % together with the analogue section where  $X = \text{Ni}$  or  $\text{Al}$ . As seen in the figure there is hardly any difference between  $\text{Cu}$  and  $\text{Ni}$  and between  $\text{Al}$  and  $\text{Ti}$ . Furthermore, the discontinuity in slope remains both for  $\text{Cu}$  and  $\text{Al}$  corresponding to the points  $N$  and  $A$  in Fig. 14, respectively. As a result the surface of the  $\gamma'$  enthalpy for these two elements is folded and the fold for  $\text{Cu}$  is aligned in the "Ni direction" and for  $\text{Ti}$  in the "Al direction." This result explains why the solubility lobes of  $\gamma'$  in ternary phase diagrams extends in the "Ni direction" in the case of  $\text{Cu}$  and in the "Al direction" in the case of  $\text{Ti}$ .

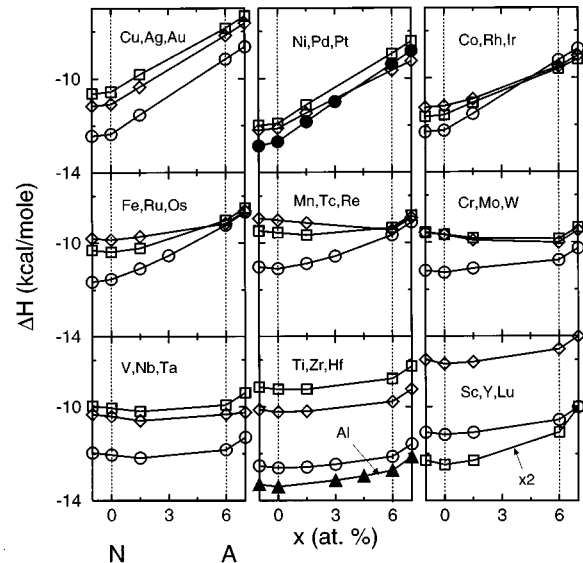


FIG. 16. Enthalpies of formation of ternary partially ordered  $\text{Ni}_{69+x}\text{Al}_{25-x}\text{X}_6$  alloys as functions of  $x$ . Open circles are the results for  $3d$  metals, open squares for  $4d$  metals, and open diamonds for  $5d$  metals. Solid circles in the upper panel are the results for  $X = \text{Ni}$ , while solid triangles in the lower panel are the results for  $\text{Al}$ . Dotted lines show the region of quasistoichiometric alloy compositions.

Finally, one may see in the figure that the discontinuous slope is absent for  $\text{Fe}$  and in this case the  $\gamma'$  phase boundary may therefore be extremely sensitive to a number of factors. Hence, it is hardly surprising that the experimental data concerning the direction of the  $\gamma'$  solubility lobe in  $\text{Ni-Al-Fe}$  ternary system are inconsistent.<sup>1,47,48</sup>

The importance of this result is the fact that while such a behavior of the enthalpy of formation is quite expected for  $\text{Ti}$ , it cannot be predicted for  $\text{Cu}$  solely from the knowledge that  $\text{Cu}$  exhibits only weak  $\text{Ni}$  site preference in the  $\text{Ni}_3\text{Al}$ . Hence, there exists no unambiguous connection between the direction of the solubility lobe and the site substitution behavior and therefore the alignment of the solubility lobe along either the "Ni direction" or the "Al direction" cannot be considered as proof of a strong  $\text{Ni}$  or  $\text{Al}$  site preference.

In Fig. 16 we show the quasibinary sections  $\bar{c}_X = 6$  at. % of the enthalpy of formation surfaces for all transition and noble metals including  $\text{Ni}$  and  $\text{Al}$ . One observes that the sections for  $\text{Cu}, \text{Ag}, \text{Au}, \text{Pd}, \text{Pt},$  and  $\text{Co}$  are very similar to that of  $\text{Ni}$  (solid circles) while the sections for  $\text{V}, \text{Nb}, \text{Ta}, \text{Ti}, \text{Zr}, \text{Hf}, \text{Sc}, \text{Y},$  and  $\text{Lu}$  are very similar to that of  $\text{Al}$  (solid triangles). Hence one may expect the solubility lobe of the  $\gamma'$  phase for the elements  $\text{Cu}, \text{Ag}, \text{Au}, \text{Pd}, \text{Pt},$  and  $\text{Co}$  to be aligned along the "Ni direction" and that of  $\text{V}, \text{Nb}, \text{Ta}, \text{Ti}, \text{Zr}, \text{Hf}, \text{Sc}, \text{Y},$  and  $\text{Lu}$  to be aligned along the "Al direction." These conclusions are in complete agreement with existing phase diagrams.<sup>47</sup>

## VII. SUMMARY

We present and discuss a technique based on first-principles calculations of the total energy of ternary partially ordered alloys which may be used to calculate site substitution behavior of ternary additions to binary ordered alloys

with two types of sublattices as well as in general investigations of the alloying behavior of many-component partially ordered alloys. Here, the technique is used to study the site preference of transition and noble metals in  $\text{Ni}_3\text{Al}$ . Our results show that in contrast to previous interpretations of available experimental data none of the transition or noble metals exhibits strong preference for Ni sites although a few exhibit weak Ni preference. We do, however, find that the metals Sc, Ti, V, Cr, Y, Zr, Nb, Mo, Tc, Lu, Hf, Ta, W, Re, and Os exhibit strong Al site preference in the dilute limit of the ternary addition to quasistoichiometric  $\gamma'$   $\text{Ni}_3\text{Al}$  at 0 K.

We show that the observed simple trends in the site substitution behavior of the transition metals, i.e., the decrease of Al site preference with increasing atomic number across a row of the Periodic Table and the increase of Al site preference with atomic number down a column of the Periodic Table, are driven by the Ni–transition-metal interactions governed by the electronic properties of the added species in the form of  $d$ -occupation number and  $d$ -band width. Further, the weakening of the Ni site preference observed in the noble metals is shown to be a consequence of the reduced Al–noble-metal interactions relative to the Al–transition-metal interactions.

We emphasize that the theoretical classification of site occupation behavior presented in Fig. 4 is only strictly valid in the dilute limit and at 0 K and we point to composition and temperature effects which must be considered before a consistent interpretation of experimental results can be obtained. In particular, we show that an alloying element which according to the classification exhibits strong Al site preference may occupy Ni sites even in the case of quasistoichiometric ternary alloys. This may be the case for Cr, Tc, Re, and Os. Further, we show that elements which according to the classification exhibit only weak Al or Ni site preference may in Ni or Al deficient alloys exhibit site occupation reversal with increasing temperature whereby they appear to have strong Al or Ni site preference. We find that the temperature where the reversal transition sets in may be quite close to 0 K and that the lower the concentration of the added species the sharper the reversal transition. In addition, we demonstrate that even if a ternary addition does not exhibit any site preference at 0 K, as in the case of Fe, site occupation reversal may still be observed in  $\text{Ni}_3\text{Al}$  due to the asymmetrical form of the entropy. Reversal of site occupation may occur for Mn, Fe, Co, Cu, Ru, Rh, Pd, Ag, Ir, Pt, and Au.

Finally, on the basis of the calculated enthalpies of formation of ternary and binary  $\gamma'$  we have estimated the direction of the solubility lobe of  $\gamma'$  in the ternary phase diagrams. We show that although Cu, Pd, and Co exhibit only weak Ni site preference the solubility lobe of the  $\gamma'$  phase should be oriented in the “Ni direction” as is in fact observed experimentally.

#### ACKNOWLEDGMENTS

We would like to thank Professor A.G. Khachaturyan for a helpful discussion and Dr. A. Yu. Lozovoi for some useful comments. Center for Atomic-scale Materials Physics is sponsored by the Danish National Research Foundation.

#### APPENDIX: ORDERING ENERGY IN THE CONCENTRATION WAVE METHOD

Here we define the ordering energy within the concentration wave method<sup>49</sup> and give a general expression for the ordering energy in terms of pairwise interactions. The starting point is the Hamiltonian for a  $t$ -component alloy

$$H = \frac{1}{2} \sum_{R \neq R'} \sum_{i,j=1}^t v_{ij}(R, R') c_i(R) c_j(R'), \quad (\text{A1})$$

where  $v_{ij}(R, R')$  is the interatomic pair potential between  $i$  and  $j$  atoms being in positions  $R$  and  $R'$ , and  $c_i(R)$  the occupation number which is 1 if site  $R$  is occupied by an  $i$  atom and 0 otherwise.

It is more convenient to write the configuration dependent part of the Hamiltonian in terms of concentration fluctuations  $\delta c_i(R) = \bar{c}_i - c_i(R)$  at site  $R$ :

$$H_{\text{conf}} = \frac{1}{2} \sum_{i,j=1}^{t-1} \left\{ \sum_{R,R'} V_{ijt}(R, R') \delta c_i(R) \delta c_j(R') - \sum_R \delta c_i(R) \delta c_j(R) V_{ijt}(R, R) \right\}. \quad (\text{A2})$$

Here  $V_{ijt}$  are generalized effective pair interactions (EPI)

$$V_{ijt} = v_{ij} + v_{it} - v_{it} - v_{jt}, \quad (\text{A3})$$

connected with ordinary EPI  $\tilde{V}_{ij}$  by the relations

$$\tilde{V}_{ij} = V_{ijj} = V_{jji}; \quad (\text{A4})$$

$$V_{ijt} = \frac{1}{2} [\tilde{V}_{jt} + \tilde{V}_{it} - \tilde{V}_{ij}]. \quad (\text{A5})$$

Determining the concentration wave of an  $i$  component as the Fourier transformation of  $\delta c_i(R)$

$$c_q^i = \sum_R \delta c_i(R) e^{iqR}, \quad (\text{A6})$$

one may write the configuration energy of an alloy as

$$E_{\text{conf}} = \frac{1}{2} \sum_{i,j=1}^{t-1} \left\{ \frac{\Omega}{(2\pi)^3} \int_{\text{BZ}} dq V_{ijt}(q) c_q^i c_q^{*j} - (\delta_{ij} \bar{c}_i - \bar{c}_i \bar{c}_j) V_{ijt}(R=0) \right\}, \quad (\text{A7})$$

where  $V_{ijt}(q)$  is the Fourier component of the generalized EPI,  $\Omega$  the volume of unit cell, and  $V_{ijt}(R=0) \equiv V_{ijt}(R, R)$  is defined as

$$V_{ijt}(R=0) = \frac{\Omega}{(2\pi)^3} \int_{\text{BZ}} dq V_{ijt}(q). \quad (\text{A8})$$

In general the amplitudes of the concentration waves obey the following normalization condition,

$$\frac{\Omega}{(2\pi)^3} \int_{\text{BZ}} dq c_q^i c_q^{*j} = \delta_{ij} \bar{c}_i - \bar{c}_i \bar{c}_j, \quad (\text{A9})$$

and using definition (A6) one finds

$$c_q^i c_q^{*j} = \delta_{ij} \bar{c}_i - \bar{c}_i \bar{c}_j + \sum_{R \neq R'} [c_i(R) c_j(R') - \bar{c}_i \bar{c}_j(R')] - \bar{c}_j c_i(R) + \bar{c}_i \bar{c}_j] e^{iq(R-R')}. \quad (\text{A10})$$

In the case of completely random alloys the last term in Eq. (A10) is equal to 0, and so

$$c_q^i c_q^{*j} = \delta_{ij} \bar{c}_i - \bar{c}_i \bar{c}_j, \quad (\text{A11})$$

i.e., the amplitude of concentration waves does not depend on  $q$  and the completely random alloy may be considered a superposition of concentration waves with all wave vectors constituting a homogeneous background. This leads to the obvious result, that the configuration energy of a completely random alloy is equal to zero, i.e.,

$$E_{\text{conf}}^{\text{rand}} = \frac{1}{2} \sum_{i,j=1}^{t-1} \left\{ \frac{\Omega}{(2\pi)^3} \int_{\text{BZ}} dq V_{ijt}(q) (\delta_{ij} \bar{c}_i - \bar{c}_i \bar{c}_j) - (\delta_{ij} \bar{c}_i - \bar{c}_i \bar{c}_j) V_{ijt}(R=0) \right\} = 0. \quad (\text{A12})$$

Now we may find the ordering energy in the mean-field approximation of a  $t$ -component alloy with two types of non-equivalent sublattices,  $A_k B_m$ . In this case one finds that there are some additional concentration waves providing the corresponding symmetry of the ordering phase,<sup>49</sup> so that the average value of the concentration at the sites is

$$\langle c_i(R) \rangle = \bar{c}_i + \eta_i \epsilon(R) = \bar{c}_i + \eta_i \gamma \frac{1}{2} \sum_{j_s} [\exp(ik_{j_s} R) + \text{c.c.}], \quad (\text{A13})$$

where sum is taken over members of a star of the special point  $k_s$  corresponding to a given ordered phase,  $\gamma$  is the normalization factor, and  $\eta_i$  is the long-range order parameter of the  $i$  component which we will define here as  $c_i(A) - c_i(B)$ .

Inserting Eq. (A13) into Eq. (A10) one finds the following relationship for the amplitudes of concentration waves in the case of partially ordered alloy without SRO effects on each individual sublattice:

$$c_q^i c_q^{*j} = \delta_{ij} \bar{c}_i - \bar{c}_i \bar{c}_j + \gamma^2 \eta_i \eta_j \sum_{j_s} [S(k_{j_s} - q) S^*(k_{j_s} - q) - 1], \quad (\text{A14})$$

where  $S(k_{j_s} - q)$  is the structure factor  $\sum_R \exp[i(k_{j_s} - q)R]$ . Noting that the normalizing factor  $\gamma$  should provide the following values of  $\epsilon(R)$  in the  $A$  and  $B$  sites in the completely ordered state:

$$\epsilon(R=A) = \frac{m}{k+m} \equiv \xi_B; \quad \epsilon(R=B) = \frac{k}{k+m} \equiv \xi_A, \quad (\text{A15})$$

one finds that  $\gamma = 1/(k+m)$  and the number of the members of the star should be equal  $km$ , and thus

$$c_q^i c_q^{*j} = \delta_{ij} \bar{c}_i - \bar{c}_i \bar{c}_j + \eta_i \eta_j \left[ \frac{1}{(k+m)^2} \sum_{j_s} S(k_{j_s} - q) \times S^*(k_{j_s} - q) - \xi_A \xi_B \right]. \quad (\text{A16})$$

The physical meaning of the last term in Eq. (A16) is transparent: The homogeneous background of the concentration waves corresponding to the completely random state is reduced by the appearance of the new concentration waves which establish order on the underlying lattice, and thus Eq. (A16) satisfies the normalization condition (A9). It may be also shown that in the completely ordered state the only remaining concentration waves are the waves with wave vectors  $k_{j_s}$ .

Inserting Eq. (A16) into Eq. (A7) one finds the ordering energy per atom

$$E_{\text{ord}} = \frac{1}{2} \xi_A \xi_B \sum_{i,j=1}^{t-1} [V_{ijt}(k_s) - V_{ijt}(R=0)] \eta_i \eta_j, \quad (\text{A17})$$

which for ternary ordered alloys with definitions (1) has exactly the form of Eq. (14)

$$E_{\text{ord}} = \frac{1}{2} \xi_A \xi_B [W_{AAX}(k_s) \eta_A^2 + W_{BBX}(k_s) \eta_B^2 - 2W_{ABX}(k_s) \eta_A \eta_B], \quad (\text{A18})$$

where  $W_{ijt}(k_s) = V_{ijt}(k_s) - V_{ijt}(R=0)$ .

<sup>1</sup>R. W. Guard and J. H. Westbrook, Trans. Metall. Soc. AIME **215**, 807 (1959).

<sup>2</sup>R. D. Rawlings and A. E. Staton-Bevan, J. Mater. Res. **6**, 505 (1975).

<sup>3</sup>H. Lin and D. Pope, J. Mater. Res. **5**, 763 (1990).

<sup>4</sup>A. Marty, M. Bessiere, F. Bley, Y. Calvayrac, and S. Lefebvre, Acta Metall. Mater. **38**, 345 (1990).

<sup>5</sup>P. R. Munroe and I. Baker, J. Mater. Res. **6**, 943 (1991).

<sup>6</sup>A. Chiba, D. Shindo, and S. Hanada, Acta Metall. Mater. **39**, 13 (1991).

<sup>7</sup>K. Hono, H. Numakura, I. A. Szabo, A. Chiba, and T. Sakurai, Surf. Sci. **266**, 358 (1992).

<sup>8</sup>M. K. Miller and J. A. Horton, in *High Temperature Ordered*

*Intermetallic Alloys II*, edited by N. S. Stoloff, C. C. Koch, C. T. Liu, and O. Izumi, MRS Symposia Proceedings No. 81 (Materials Research Society, Pittsburgh, 1987), p. 165.

<sup>9</sup>H. Lin, L. E. Seiberling, P. F. Lyman, and D. P. Pope, in *High Temperature Ordered Intermetallic Alloys II*, edited by N. S. Stoloff, C. C. Koch, C. T. Liu, and O. Izumi, MRS Symposia Proceedings No. 81 (Materials Research Society, Pittsburgh, 1987), p. 117.

<sup>10</sup>H. G. Bohn, R. Schumacher, and R. J. Vianden, in *High Temperature Ordered Intermetallic Alloys II*, edited by N. S. Stoloff, C. C. Koch, C. T. Liu, and O. Izumi, MRS Symposia Proceedings No. 81 (Materials Research Society, Pittsburgh, 1987), p. 123.

- <sup>11</sup>H. G. Bohn, J. W. Williams, J. H. Barret, and C. T. Liu, in *High Temperature Ordered Intermetallic Alloys II*, edited by N. S. Stoloff, C. C. Koch, C. T. Liu, and O. Izumi, MRS Symposia Proceedings No. 81 (Materials Research Society, Pittsburg, 1987), p. 127.
- <sup>12</sup>S. Ochiai, Y. Oya, and T. Suzuki, *Acta Metall.* **32**, 289 (1984).
- <sup>13</sup>J.-H. Xu, T. Oguchi, and A. J. Freeman, *Phys. Rev. B* **36**, 4186 (1987).
- <sup>14</sup>Y. P. Wu, N. C. Tso, J. M. Sanchez, and J. K. Tien, *Acta Metall.* **37**, 2835 (1989).
- <sup>15</sup>M. Enomoto and H. Harada, *Met. Trans.* **20A**, 649 (1989).
- <sup>16</sup>A. Marty, Y. Calvayrac, F. Guillet, and P. Cenedese, *Phys. Rev. B* **44**, 11 640 (1991).
- <sup>17</sup>C. Wolverton and D. de Fontaine, *Phys. Rev. B* **49**, 12 351 (1994).
- <sup>18</sup>M. H. F. Sluiter and Y. Kawazoe, *Phys. Rev. B* **51**, 4062 (1995); M. H. F. Sluiter and Y. Kawazoe, *Sci. Rep. RITU A40* (1995), p. 301; M. H. F. Sluiter, M. Takahashi, and Y. Kawazoe, in *High-Temperature Ordered Intermetallic Alloys VI*, edited by J. Horton, S. Hanada, I. Baker, R. D. Noebe, and D. Schwartz, MRS Symposia Proceedings No. 364 (Materials Research Society, Pittsburgh, 1995), p. 58; M. H. F. Sluiter, M. Takahashi, and Y. Kawazoe, *Acta Metall. Mater.* (to be published).
- <sup>19</sup>A. V. Ruban, I. A. Abrikosov, and H. L. Skriver, *Phys. Rev. B* **51**, 12 958 (1995).
- <sup>20</sup>A. V. Ruban and H. L. Skriver, *Solid State Commun.* **49**, 813 (1996).
- <sup>21</sup>J. Friedel, in *The Physics of Metals*, edited by J. M. Ziman (Cambridge University Press, Cambridge, England, 1969), p. 494.
- <sup>22</sup>Z. W. Lu, S.-H. Wei, and A. Zunger, *Phys. Rev. B* **45**, 10 314 (1992).
- <sup>23</sup>C. Wolverton and A. Zunger, *Phys. Rev. B* **51**, 6876 (1995).
- <sup>24</sup>M. A. Krivoglaz, *Sov. J. Phys. Chem.* **31**, 1930 (1957).
- <sup>25</sup>A. E. Carlsson, *Phys. Rev. B* **40**, 912 (1989).
- <sup>26</sup>The relation to  $J$  defined by Marty *et al.* (Ref. 16) and  $S$  defined by Sluiter and Kawazoe (Ref. 18) is  $2\tilde{E}_{\text{Ni} \rightarrow \text{Al}}^X = -J - 1 = S + 1$ .
- <sup>27</sup>O.K. Andersen, O. Jepsen, and D. Glötzel, in *Highlights of Condensed-Matter Theory*, edited by F. Bassani, F. Fumi, and M. P. Tosi (North-Holland, New York, 1985).
- <sup>28</sup>O.K. Andersen and O. Jepsen, *Phys. Rev. Lett.* **53**, 2571 (1984).
- <sup>29</sup>O. K. Andersen, Z. Pawlowska, and O. Jepsen, *Phys. Rev. B* **34**, 5253 (1986).
- <sup>30</sup>J. Perdew and A. Zunger, *Phys. Rev. B* **23**, 5048 (1981).
- <sup>31</sup>D. M. Ceperley and B. J. Alder, *Phys. Rev. Lett.* **45**, 566 (1980).
- <sup>32</sup>S. H. Vosko, L. Wilk, and M. Nusair, *Can. J. Phys.* **58**, 1200 (1980).
- <sup>33</sup>V. Kumar, D. Kumar, and S. K. Joshi, *Phys. Rev. B* **19**, 1954 (1979).
- <sup>34</sup>V. L. Moruzzi, J. F. Janak, and K. Schwarz, *Phys. Rev. B* **37**, 790 (1988).
- <sup>35</sup>P. A. Korzhavyi, A. V. Ruban, I. A. Abrikosov, and H. L. Skriver, *Phys. Rev. B* **51**, 5773 (1995).
- <sup>36</sup>J. Zou and A. E. Carlsson, *Phys. Rev. Lett.* **70**, 3748 (1993).
- <sup>37</sup>R. Phillips, J. Zou, A. E. Carlsson, and M. Widom, *Phys. Rev. B* **49**, 9322 (1994).
- <sup>38</sup>J. Zou and C. L. Fu, *Phys. Rev. B* **51**, 169 (1995).
- <sup>39</sup>J. Zou and C. L. Fu, *Phys. Rev. B* **51**, 2115 (1995).
- <sup>40</sup>At  $T=0$  K the Gorsky-Bragg-Williams equations (24) cannot be solved simultaneously because of Eq. (10) which is correct at any point in the LRO space. In fact, due to the limited configuration space, the shaded area in Fig. 1, it may happen that none of the equations may be satisfied in which case the equilibrium state is at one of the points  $B$ ,  $C$ , or  $D$ . If a single equation is satisfied the equilibrium state will be on one of the two segments  $BC$  and  $CD$ .
- <sup>41</sup>Strictly speaking both LRO parameters may have negative values and the point  $D$  may be below the  $\eta_{\text{Ni}}$  axis. However, for small concentration of  $X$  this is possible only in the case of off-stoichiometric alloy compositions. For instance, to satisfy this condition if  $\bar{c}_X = 12$  at. % the Ni concentration should be less than 36 at. % ( $< 3\bar{c}_X$ ) and the Al concentration greater than 48 at. % which is too far from their binary stoichiometric values. On the other hand, for quasistoichiometric alloy compositions the point  $D$  may be below  $\eta_{\text{Ni}}$  axis only if  $\bar{c}_X > 18.75$  at. %.
- <sup>42</sup>M. H. F. Sluiter, K. Esfarjani, and Y. Kawazoe, *Phys. Rev. Lett.* **75**, 3142 (1995).
- <sup>43</sup>A. V. Karg, D. E. Fornwalt, and O. H. Kriege, *J. Inst. Met.* **99**, 301 (1971).
- <sup>44</sup>R. Kikuchi and J. L. Murray, *CALPHAD* **9**, 311 (1985).
- <sup>45</sup>R. W. Kahn, P. A. Siemens, J. E. Geiger, and P. Bardhan, *Acta Metall.* **35**, 2737 (1987).
- <sup>46</sup>A. E. Carlsson and J. M. Sanchez, *Solid State Commun.* **65**, 527 (1988).
- <sup>47</sup>*Ternary Alloys, a compendium of evaluated constitutional data and phase diagrams*, edited by G. Petzow and G. Effenberg (VCH Publishers, New York, 1993), Vols. 4–8.
- <sup>48</sup>E. S. Machlin and J. Shao, *Scr. Metall.* **11**, 859 (1977).
- <sup>49</sup>A.G. Khachaturyan, *The Theory of Structural Transformations in Solids* (Wiley, New York, 1983).